

ON CHARGE-3 CYCLIC MONOPOLES

H. W. BRADEN, ANTONELLA D'AVANZO, AND V. Z. ENOLSKI

ABSTRACT. We determine the spectral curve of charge 3 BPS $su(2)$ monopoles with C_3 cyclic symmetry. The symmetry means that the genus 4 spectral curve covers a (Toda) spectral curve of genus 2. A well adapted homology basis is presented enabling the theta functions and monopole data of the genus 4 curve to be given in terms of genus 2 data. The Richelot correspondence, a generalization of the arithmetic mean, is used to solve for this genus 2 curve. Results of other approaches are compared.

CONTENTS

1. Introduction	1
2. The curve	5
2.1. Branchpoints and monodromy	5
2.2. The quotient with respect to C_3	6
2.3. Homology bases	8
2.4. Period matrices	13
2.5. The Fay-Accola theorem	16
2.6. The vector of Riemann constants	17
3. The Ercolani-Sinha conditions	19
4. The AGM method	20
4.1. AGM: the elliptic case	20
4.2. Richelot and Humbert: the genus 2 case.	21
4.3. Generalisation to the genus 2 case with complex conjugate roots	25
5. Solving the Ercolani-Sinha constraints via the AGM	27
5.1. Numerical solutions	27
6. Discussion	29
Acknowledgements	32
References	33

1. INTRODUCTION

The first order Bogomolny equations,

$$(1.1) \quad B_i = \frac{1}{2} \sum_{j,k=1}^3 \epsilon_{ijk} F^{jk} = D_i \Phi,$$

are rather ubiquitous. They arose while studying a limit of Yang-Mills-Higgs gauge theory in three space dimensions in which the the Higgs potential is removed but a remnant of this remains in the boundary conditions associated with (1.1). Here F_{ij} is the field strength

Date: October 26, 2018.

associated to a gauge field A , and Φ is the Higgs field. The same equations may also be viewed as a dimensional reduction of the four dimensional self-dual equations upon setting all functions independent of x_4 and identifying $\Phi = A_4$; they are also encountered in supersymmetric theories when requiring certain field configurations to preserve some fraction of supersymmetry. Just as the self-duality equations admit instanton solutions in four dimensions, the Bogomolny equations possess topological soliton solutions with particle-like properties, known as magnetic monopoles, and these have been the subject of considerable interest over the years [MS04]. Early on a curve $\hat{\mathcal{C}}$ was found to be associated to these BPS monopoles. Indeed the same curve arose by (at least) two different routes both with origins in instanton theory. Whilst considering the Atiyah-Ward instanton ansatz in the monopole setting Corrigan and Goddard [CG81] encountered $\hat{\mathcal{C}}$ and this was given a twistorial description by Hitchin [Hit82]. Just as Ward's twistor transform relates instanton solutions on \mathbb{R}^4 to certain holomorphic vector bundles over the twistor space \mathbb{CP}^3 , Hitchin showed that the dimensional reduction leading to BPS monopoles could be made at the twistor level as well and the curve $\hat{\mathcal{C}}$ naturally lies in mini-twistor space, $\hat{\mathcal{C}} \subset \mathbb{TP}^1$. The second appearance of the curve $\hat{\mathcal{C}}$ is closely connected with integrable systems. Nahm gave a transform of the ADHM instanton construction to produce BPS monopoles [Nah82] and the resulting Nahm's equations have Lax form with corresponding spectral curve $\hat{\mathcal{C}}$. Hitchin [Hit83] proved that all monopoles could be obtained by Nahm's approach provided the curve $\hat{\mathcal{C}}$ was subject to certain nonsingularity conditions. Bringing methods from integrable systems to bear upon the construction of solutions to Nahm's equations for the gauge group $SU(2)$ Ercolani and Sinha [ES89] later showed how one could solve (a gauge transform of) the Nahm equations in terms of a Baker-Akhiezer function for the curve $\hat{\mathcal{C}}$. Thus given a curve $\hat{\mathcal{C}}$ the machinery of integrable systems allows one (in principle) to construct solutions to Nahm's equations and thence monopoles [BE09A].

The problem in the approach just described, and to which this paper is devoted, is in constructing the curve $\hat{\mathcal{C}}$: some of the conditions necessary for the regularity of solutions just alluded to impose transcendental constraints on $\hat{\mathcal{C}}$, and we presently lack analytic means for solving these. One such constraint comes about by requiring the periods of a meromorphic differential on $\hat{\mathcal{C}}$ to be specified. This type of constraint arises in many other settings as well, for example when specifying the filling fractions of a curve in the AdS/CFT correspondence [KMMZ], finding closed geodesics on an ellipsoid [AF06] or constructing harmonic maps $T^2 \rightarrow S^3$ [Hit90]. The second type of constraint is that the linear flow on the Jacobian of $\hat{\mathcal{C}}$ corresponding to the integrable motion only intersects the theta divisor in a prescribed manner; equivalently this may be expressed as the vanishing of a real one parameter family of cohomologies of certain line bundles on $\hat{\mathcal{C}}$. While techniques exist that count the number of intersections of a complex line with the theta divisor we are unaware of anything comparable in the real setting [BE09B]. Thus the application of integrable systems techniques to the construction of monopoles (and indeed more generally) encounters two types of problem that each merit further study.

In the present paper we will simplify then solve these constraints by imposing spatial symmetries on the monopole. Imposing symmetry reduces the number of constraints to be solved for and here we shall focus on charge 3 monopoles with cyclic symmetry \mathbf{C}_3 . The spectral curve of a charge n monopole may be expressed in the form

$$P(\eta, \zeta) := \eta^n + \eta^{n-1}a_1(\zeta) + \dots + \eta^r a_{n-r}(\zeta) + \dots + \eta a_{n-1}(\zeta) + a_n(\zeta) = 0,$$

where $a_r(\zeta)$ (for $1 \leq r \leq n$) is a polynomial in ζ of maximum degree $2r$. Hitchin's construction involves three constraints on the curve. The first **(H1)** requires the curve $\hat{\mathcal{C}}$ to be real

with respect to the standard real structure on $T\mathbb{P}^1$,

$$(1.2) \quad \tau : (\zeta, \eta) \mapsto \left(-\frac{1}{\bar{\zeta}}, -\frac{\bar{\eta}}{\zeta^2}\right),$$

the anti-holomorphic involution defined by reversing the orientation of the lines in \mathbb{R}^3 . As a consequence the coefficients of the curve satisfy $a_r(\zeta) = (-1)^r \zeta^{2r} \overline{a_r(-1/\bar{\zeta})}$. Imposing spatial symmetries via fractional linear transformations of $T\mathbb{P}^1$ simplifies the curve. Long ago monopoles of charge n with cyclic symmetry \mathbb{C}_n were shown to exist [OR82] and these correspond to curves invariant under $(\eta, \zeta) \rightarrow (\omega\eta, \omega\zeta)$ (where $\omega = \exp(2i\pi/n)$). Imposing Hitchin's reality conditions and centering the monopole (setting $a_1 = 0$) then gives us the \mathbb{C}_n symmetric spectral curve in the form

$$\eta^n + a_2\eta^{n-2}\zeta^2 + \dots + a_n\zeta^n + \beta\zeta^{2n} + (-1)^n\bar{\beta} = 0, \quad a_i \in \mathbf{R}.$$

By an overall rotation we may choose β real and so the charge 3 spectral curves $\hat{\mathcal{C}}$ we will focus on in this paper have the form

$$(1.3) \quad \eta^3 + \alpha\eta\zeta^2 + \beta\zeta^6 + \gamma\zeta^3 - \beta = 0.$$

The remaining two constraints of Hitchin on this curve are the transcendental constraints referred to above. The first of these (**H2**) may be expressed in the following manner [HMR00]: given a canonical homology basis $\{\hat{\mathbf{a}}_\mu, \hat{\mathbf{b}}_\mu\}$ for the curve $\hat{\mathcal{C}}$ there exists a 1-cycle $\hat{\mathbf{e}}\mathbf{s} = \mathbf{n}\cdot\hat{\mathbf{a}} + \mathbf{m}\cdot\hat{\mathbf{b}}$ such that for every holomorphic differential

$$(1.4) \quad \Omega = \frac{\beta_0\eta^{n-2} + \beta_1(\zeta)\eta^{n-3} + \dots + \beta_{n-2}(\zeta)}{\partial\mathcal{P}/\partial\eta} d\zeta, \quad \oint_{\hat{\mathbf{e}}\mathbf{s}} \Omega = -2\beta_0.$$

Dually the vector

$$\hat{\mathbf{U}} = \frac{1}{2}\mathbf{n} + \frac{1}{2}\hat{\tau}\mathbf{m}$$

(where $\hat{\tau}$ is the period matrix of $\hat{\mathcal{C}}$) is a half-period. The vector $\hat{\mathbf{U}}$ is known as the Ercolani-Sinha vector [ES89] and may be expressed as the periods of a meromorphic differential. These conditions, known as the Ercolani-Sinha constraints, impose $(n-1)^2$ (the genus of $\hat{\mathcal{C}}$) *transcendental constraints* on the curve. The remaining constraint (**H3**) is that for a special vector $\widetilde{\mathbf{K}}$ in the Jacobian the linear flow $\lambda\hat{\mathbf{U}} - \widetilde{\mathbf{K}}$ intersects the theta divisor only at $\lambda = 0$ and 2. The consequences of assuming symmetry is that the spectral curve covers another curve, the quotient curve by the symmetry. In the case of cyclic symmetry we have an n -fold unbranched cover $\pi : \hat{\mathcal{C}} \rightarrow \mathcal{C}$ of a hyperelliptic curve of genus $n-1$ which is the spectral curve of the a_n affine Toda system, and [Bra10] shows how both the constraints (**H2,3**) reduce to become constraints on the reduced curve. In particular

$$\lambda\hat{\mathbf{U}} - \widetilde{\mathbf{K}} = \pi^*(\lambda\mathbf{U} - \mathbf{K}_{\infty+} + e).$$

where \mathbf{U} expresses the Ercolani-Sinha constraints of the curve \mathcal{C} and the other quantities will be defined later. Thus in this paper we have a 3-fold unbranched cover of the of the curve \mathcal{C} given by

$$(1.5) \quad y^2 = (x^3 + \alpha x + \gamma)^2 + 4\beta^2.$$

To solve the remaining transcendental constraints for the reduced curve \mathcal{C} we now use several pieces of research. First the work of [BE06, BE09B]¹ identifies the solutions of (1.4)

¹The first of these papers consisted of two parts that have been separately published as [BE10A, BE10B].

for the class of curves (1.3) with $\alpha = 0$ and [BE09B] shows that the only solutions of the Hitchin constraints are for the curves

$$(1.6) \quad \eta^3 + \chi(\zeta^6 \pm 5\sqrt{2}\zeta^3 - 1) = 0, \quad \chi^{\frac{1}{3}} = -\frac{1}{6} \frac{\Gamma(\frac{1}{6})\Gamma(\frac{1}{3})}{2^{\frac{1}{6}}\pi^{\frac{1}{2}}}.$$

These correspond to tetrahedrally symmetric monopoles and for each sign of $\pm 5\sqrt{2}$ there is a unique vector \widehat{U} . Next we use the work of [HMM95]. Here cyclically symmetric monopoles (and more generally, those with Platonic spatial symmetries) were reconsidered from a variety of perspectives. Cyclically symmetric monopoles form 4-dimensional totally geodesic submanifolds \mathcal{M}_n^l of the full moduli space of charge n monopoles, where $0 \leq l < n$. Ignoring the rotational degrees of freedom these then yield one dimensional submanifolds. By considering the rational map description of these monopoles Hitchin, Manton and Murray were able to further specify the \mathcal{M}_n^l which may be viewed as orbits of geodesic monopole scattering. For charge 3 there were five loci of spectral curves of the form (1.3). Of these loci, four were isomorphic: at one end asymptotically one has $\alpha^3 = 27\beta^2$ (with β of either sign) and $\gamma = 0$ while at the other end $\alpha = \pi^2/4 - 3b^2$, $\beta = 0$ and $\gamma = 2b(b^2 + \pi^2/4)$ (with b of either sign). Half-way along this is the tetrahedrally symmetric monopole, the four loci corresponding to four distinct orientations of the tetrahedron. The final locus corresponds to the family of curves with $\gamma = 0$ and where the symmetry is enlarged to the dihedral symmetry D_3 : asymptotically we have $\alpha^3 = 27\beta^2$ (with β large and positive at one end and negative at the other) and half-way along this there is the axisymmetric monopole. We use this work as follows. Because the Ercolani-Sinha vector \widehat{U} is discrete, this will be constant for each of the loci emanating from the tetrahedrally symmetric points. Starting then at a point (α, β, γ) corresponding to a tetrahedrally symmetric monopole we deform away from this by solving the (reduced) Ercolani-Sinha constraint for the given fixed \widehat{U} . Thus we will obtain the loci $\gamma \neq 0$. This idea is similar to that used by Sutcliffe [Sut97] when obtaining numerical approximations to (1.3) by analysing the Nahm equations and using the fact that the tetrahedral monopole was on one of the loci. In deforming from the tetrahedrally symmetric points we will use a genus 2 variant of the arithmetic-geometric mean (AGM) (that will be described more fully in the sequel). Although this deformation is defined by the (reduced) constraint **(H2)** the ensuing loci must also satisfy **(H3)** for dimensional reasons. Thus we arrive at the spectral curves (1.3) with $\gamma \neq 0$ that describe C_3 symmetric monopoles. We remark that the $\gamma = 0$ spectral curves further cover an elliptic curve and these are amenable to a different analysis that will be given elsewhere.

An outline of the paper is as follows. In section 2 we study the curves (1.3, 1.5) in some detail determining those quantities needed to reconstruct the Baker-Akhiezer functions of the integrable systems approach. Critical here is determining an homology basis that reflects well the symmetries of the curve $\widehat{\mathcal{C}}$. Such a basis both relates and simplifies the forms of the period matrices of both $\widehat{\mathcal{C}}$ and \mathcal{C} ; it also reduces the numbers of periods to be calculated to construct the full period matrices. Perhaps the nicest feature of this homology basis (and that induced on \mathcal{C}) is that it enables us to make use of a remarkable factorisation theorem due to Accola and Fay [Acc71, Fay73] and also observed by Mumford. This allows the theta functions of $\widehat{\mathcal{C}}$ to be described in terms of the theta functions of \mathcal{C} for the parts of the Jacobian that are relevant for us [Bra10]. By the end of section 2 we have reduced the construction of cyclically invariant monopoles (with $\gamma \neq 0$) to questions about a genus two hyperelliptic curve \mathcal{C} . Section 3 then discusses the restrictions the Ercolani-Sinha constraints place on \mathcal{C} . The Ercolani-Sinha constraints are shown to reduce to the single constraint $\int_{\mathfrak{c}} dX/Y = 0$ on a scaled form of \mathcal{C} , $Y^2 = (X^3 + aX + g)^2 + 4$ (where $(a, g) := (\alpha/\beta^{2/3}, \gamma/\beta)$), and here

$\mathbf{c} := \pi(\widehat{\mathbf{cs}})$ is known. Thus the problem has become one of understanding the periods of this (scaled) genus two curve as a function of (a, g) with the Ercolani-Sinha yielding $g = g(a)$. We will solve this transcendental constraint numerically using a genus two variant of the arithmetic-geometric mean due to Richelot. Section 4 recalls this theory and describes an extension needed for the curves relevant here, which have complex conjugate branchpoints. Section 5 then implements this. We conclude with a discussion.

2. THE CURVE

In this section we consider the curve $\hat{\mathcal{C}}$ (1.3) and the quotient curve \mathcal{C} in more detail. After describing the curves we shall construct homology bases that enables several simplifications. In particular both the period matrices and vectors of Riemann constants will be described for these bases. Throughout we will set $\rho = \exp(2i\pi/3)$.

2.1. Branchpoints and monodromy. The curve (1.3) has genus 4 and is not hyperelliptic. A basis for the holomorphic differentials may be taken to be

$$(2.1) \quad \hat{\mathbf{u}}_1 = \frac{d\zeta}{3\eta^2 + \alpha\zeta^2}, \quad \hat{\mathbf{u}}_2 = \frac{\zeta d\zeta}{3\eta^2 + \alpha\zeta^2}, \quad \hat{\mathbf{u}}_3 = \frac{\zeta^2 d\zeta}{3\eta^2 + \alpha\zeta^2}, \quad \hat{\mathbf{u}}_4 = \frac{\eta d\zeta}{3\eta^2 + \alpha\zeta^2}.$$

Our curve $\hat{\mathcal{C}}$ may be viewed as a 3 sheeted cover of \mathbb{P}^1 with 12 ramification points, whose ζ -coordinates are given by

$$(2.2) \quad \begin{aligned} \hat{B}_{1,2}^\zeta &= \frac{1}{18\beta} \left(-9\gamma - 2i\sqrt{3}\alpha^{3/2} \pm \Delta_+^{1/2} \right), \\ \hat{B}_{3,4}^\zeta &= \frac{1}{18\beta} \left(-9\gamma + 2i\sqrt{3}\alpha^{3/2} \pm \Delta_-^{1/2} \right) \\ \hat{B}_{j+4k}^\zeta &= \rho^k (\hat{B}_j^\zeta)^{1/3}, \quad j = 1, \dots, 4, \quad k = 0, 1, 2, \end{aligned}$$

where

$$\Delta_\pm = 324\beta^2 - 3(2\alpha^{3/2} \pm 3i\sqrt{3}\gamma)^2.$$

In Figure 1 we give a qualitative sketch of the branchpoints; the general properties of $\hat{\mathcal{C}}$ do not change with the parameters unless $\alpha = 0$, which is a degenerate case that will be examined separately. The monodromy around each branch point is found to be

$$\hat{B}_1, \hat{B}_2, \hat{B}_7, \hat{B}_8 \longrightarrow [1, 3], \quad \hat{B}_3, \hat{B}_4, \hat{B}_9, \hat{B}_{10} \longrightarrow [1, 2], \quad \hat{B}_5, \hat{B}_6, \hat{B}_{11}, \hat{B}_{12} \longrightarrow [2, 3].$$

In addition to the real involution (1.2) and cyclic symmetry

$$(2.3) \quad \sigma : (\zeta, \eta) \rightarrow (\rho\zeta, \rho\eta)$$

the curve possesses the inversion symmetry

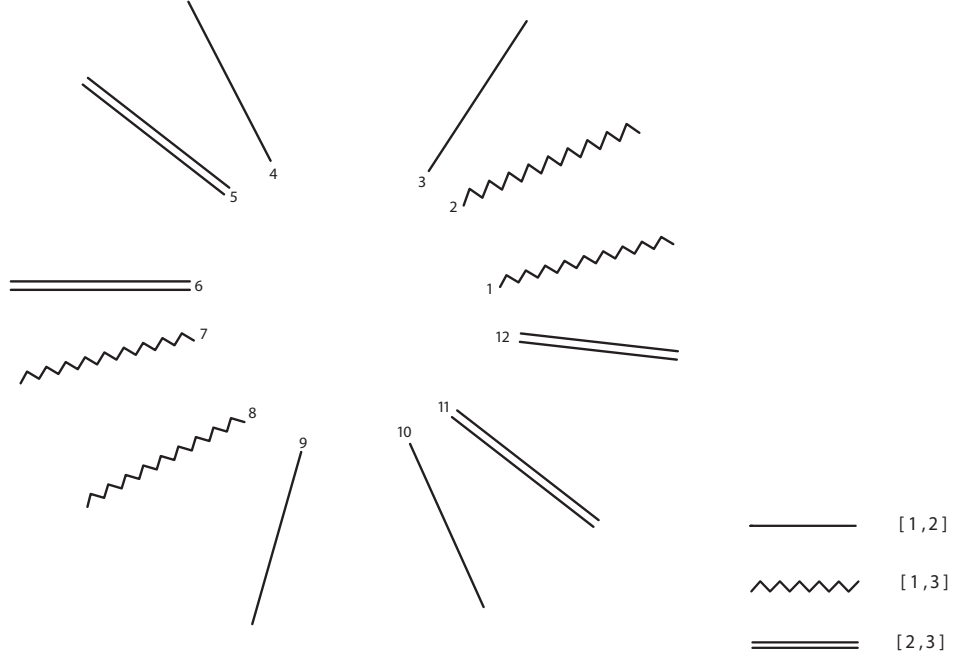
$$(2.4) \quad \phi : (\zeta, \eta) \rightarrow \left(-\frac{1}{\zeta}, -\frac{\eta}{\zeta^2} \right).$$

The branchpoints (2.2) form four orbits under the cyclic symmetry according to

$$\begin{aligned} \hat{B}_1 &\xrightarrow{\sigma} \hat{B}_5 \xrightarrow{\sigma} \hat{B}_9, & \hat{B}_2 &\xrightarrow{\sigma} \hat{B}_6 \xrightarrow{\sigma} \hat{B}_{10}, \\ \hat{B}_3 &\xrightarrow{\sigma} \hat{B}_7 \xrightarrow{\sigma} \hat{B}_{11}, & \hat{B}_4 &\xrightarrow{\sigma} \hat{B}_8 \xrightarrow{\sigma} \hat{B}_{12}. \end{aligned}$$

The case $\alpha = 0$. The case $\alpha = 0$ is the curve studied in [BE06]. The corresponding Riemann surface also has genus 4, but now only six branchpoints λ_i ($i = 1 \dots 6$),

$$\lambda_1 = \frac{1}{6\beta} \left(-3\gamma + \frac{1}{3}\Delta^{1/2} \right), \quad \lambda_4 = \frac{1}{6\beta} \left(-3\gamma - \frac{1}{3}\Delta^{1/2} \right),$$

FIGURE 1. Branchpoints and monodromy for $\hat{\mathcal{C}}$

$$\lambda_2 = \rho\lambda_1, \quad \lambda_3 = \rho^2\lambda_1, \quad \lambda_5 = \rho\lambda_4, \quad \lambda_6 = \rho^2\lambda_4,$$

where $\Delta = 27(12\beta^2 + \gamma^2)$. Indeed, letting $\alpha \rightarrow 0$ in (2.2), we see that the branchpoints \hat{B}_i collide pairwise to give the λ_i (see Figure 2). In Figure 3 we also give the monodromy which is $[1, 2, 3]$, the same for every branchpoint; this can be seen from an explicit calculation, but also by taking the limit of the monodromies of $\hat{\mathcal{C}}$.

2.2. The quotient with respect to C_3 . We may form the quotient curve $\mathcal{C} = \hat{\mathcal{C}}/\sigma$ with the covering map

$$(2.5) \quad \pi : \hat{\mathcal{C}} \longrightarrow \mathcal{C} : \quad (\zeta, \eta) \longrightarrow (x, y) = \left(\frac{\eta}{\zeta}, \beta(\zeta^3 + \frac{1}{\zeta^3}) \right).$$

and the curve \mathcal{C} is given by (1.5). It is a genus 2 (hence hyperelliptic) Riemann surface and π is an unbranched covering. Viewing \mathcal{C} as a 2-sheeted cover of the Riemann sphere, it has six branchpoints whose x -coordinates are

$$(2.6) \quad \begin{aligned} B_1^x &= \frac{1}{6} \rho \delta_-^{\frac{1}{3}} - \frac{2\rho^2 a}{\delta_-^{\frac{2}{3}}}, & B_2^x &= \frac{1}{6} \rho \delta_+^{\frac{1}{3}} - \frac{2\rho^2 a}{\delta_+^{\frac{2}{3}}}, & B_3^x &= \frac{1}{6} \delta_-^{\frac{1}{3}} - \frac{2a}{\delta_-^{\frac{2}{3}}}, \\ B_4^x &= \frac{1}{6} \delta_+^{\frac{1}{3}} - \frac{2a}{\delta_+^{\frac{2}{3}}}, & B_5^x &= \frac{1}{6} \rho^2 \delta_-^{\frac{1}{3}} - \frac{2\rho a}{\delta_-^{\frac{2}{3}}}, & B_6^x &= \frac{1}{6} \rho^2 \delta_+^{\frac{1}{3}} - \frac{2\rho a}{\delta_+^{\frac{2}{3}}}, \end{aligned}$$

where

$$\delta_{\pm} = -108\gamma - 216\beta i + 12 \sqrt{12\alpha^3 + 81(\gamma \pm 2\beta i)^2}.$$

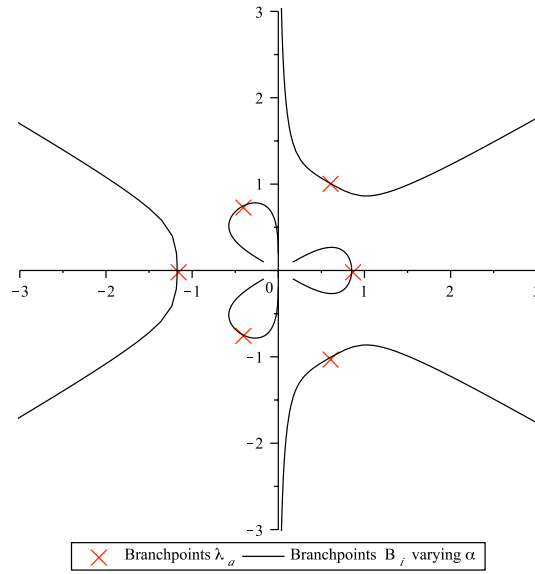


FIGURE 2. Branchpoints for $\alpha \rightarrow 0$

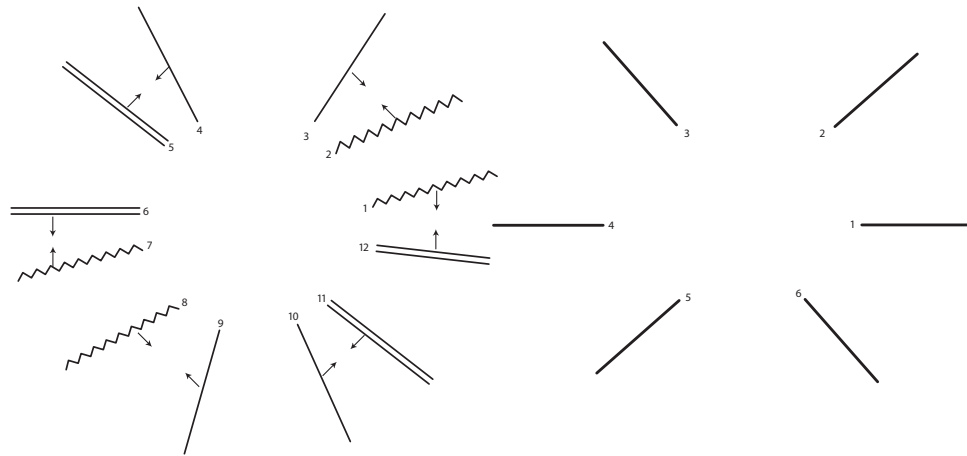
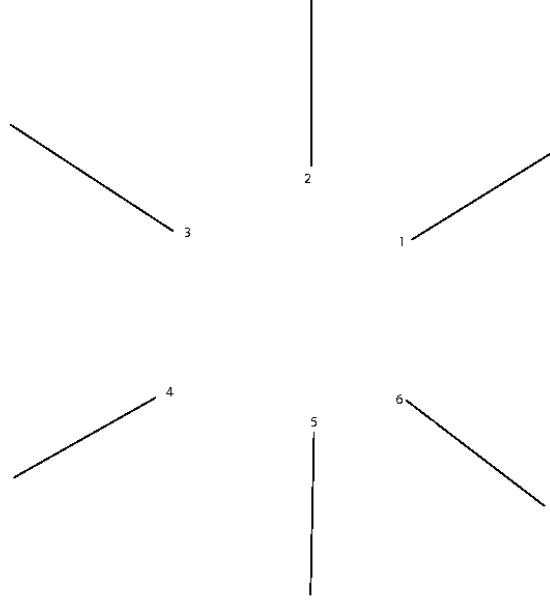


FIGURE 3. Branchpoints and monodromy for $\alpha \rightarrow 0$.

As $\delta_- = \overline{\delta_+}$, these branchpoints can be split into complex conjugate pairs

$$(2.7) \quad B_6^x = \overline{B_1^x}, \quad B_5^x = \overline{B_2^x}, \quad B_4^x = \overline{B_3^x}.$$

The branchpoints B_i are not the images of the branchpoints of $\hat{\mathcal{C}}$ under π . Figure 4 shows again a qualitative sketch of the branchpoints for the curve and their monodromy, with the same choice of parameters of Figure 1. Because the branch points are not images of those of $\hat{\mathcal{C}}$ we observe that there is little difference in the quotient curves for α equalling or differing from zero.

FIGURE 4. Branchpoints and monodromy for \mathcal{C}

A standard basis for the holomorphic differentials on \mathcal{C} is given by

$$(2.8) \quad \mathbf{u}_1 = \frac{dx}{y}, \quad \mathbf{u}_2 = \frac{x dx}{y}.$$

The differentials $\hat{\mathbf{u}}_2$ and $\hat{\mathbf{u}}_4$ on $\hat{\mathcal{C}}$ are invariant under σ and hence descend to differentials on \mathcal{C} . In fact,

$$(2.9) \quad \pi^* \mathbf{u}_1 = -3\hat{\mathbf{u}}_2, \quad \pi^* \mathbf{u}_2 = -3\hat{\mathbf{u}}_4.$$

This observation allows us to considerably simplify some integrals, and hence the period matrix.

2.3. Homology bases. By choosing an homology basis well adapted to the symmetry at hand we may simplify many things. The aim of this subsection is to construct one such basis. For the case of our unbranched cover $\pi : \hat{\mathcal{C}} \rightarrow \mathcal{C}$ it is known [Fay73] that there exists a basis $\{\hat{\mathbf{a}}_0, \hat{\mathbf{b}}_0, \hat{\mathbf{a}}_1, \hat{\mathbf{b}}_1, \hat{\mathbf{a}}_2, \hat{\mathbf{b}}_2, \hat{\mathbf{a}}_3, \hat{\mathbf{b}}_3\}$ of homology cycles for $\hat{\mathcal{C}}$ and $\{\mathbf{a}_0, \mathbf{b}_0, \mathbf{a}_1, \mathbf{b}_1, \}$ for \mathcal{C} such that (for $1 \leq j \leq 3$, $0 \leq s < 3$)

$$(2.10) \quad \sigma^s(\hat{\mathbf{a}}_0) \sim \hat{\mathbf{a}}_0, \quad \sigma^s(\hat{\mathbf{a}}_j) = \hat{\mathbf{a}}_{j+s}, \quad \sigma^s(\hat{\mathbf{b}}_0) = \hat{\mathbf{b}}_0, \quad \sigma^s(\hat{\mathbf{b}}_j) = \hat{\mathbf{b}}_{j+s},$$

$$(2.11) \quad \pi(\hat{\mathbf{a}}_0) = \mathbf{a}_0, \quad \pi(\hat{\mathbf{a}}_{j+s}) = \mathbf{a}_j, \quad \pi(\hat{\mathbf{b}}_0) = 3\mathbf{b}_0, \quad \pi(\hat{\mathbf{b}}_{j+s}) = \mathbf{b}_j.$$

Here $\sigma^s(\hat{\mathbf{a}}_0)$ is homologous to $\hat{\mathbf{a}}_0$ and indices are understood to be modulo 3. These requirements do not uniquely determine a homology basis and we may impose some extra conditions on this basis. The condition we choose (and will see is possible) is that the limit $\alpha \rightarrow 0$ of some cycles are mapped to some of the homology basis in [BE06]. This will enable us to relate the present work with [BE06] whose results we generalise. We also observe that given

two cycles $\hat{\mathbf{a}}_1, \hat{\mathbf{b}}_1$ with canonical pairing then we may simply define $\hat{\mathbf{a}}_{2,3}$ via $\hat{\mathbf{a}}_{1+s} = \sigma^s(\hat{\mathbf{a}}_1)$ (and similarly for $\hat{\mathbf{b}}_{2,3}$). Thus we seek two cycles $\hat{\mathbf{a}}_1, \hat{\mathbf{b}}_1$ such that

$$\hat{\mathbf{a}}_1^0 := \lim_{\alpha \rightarrow 0} \hat{\mathbf{a}}_1 = \mathbf{a}_1^{\text{BE06}}, \quad \hat{\mathbf{b}}_1^0 := \lim_{\alpha \rightarrow 0} \hat{\mathbf{b}}_1 = \mathbf{b}_1^{\text{BE06}}.$$

Such cycles and their corresponding images under σ are shown in Figure 5 alongside the $\alpha = 0$ limit of these. One further finds that we may choose $\hat{\mathbf{a}}_0$ such that

$$\hat{\mathbf{a}}_0^0 := \lim_{\alpha \rightarrow 0} \hat{\mathbf{a}}_0 = \mathbf{a}_4^{\text{BE06}}$$

and (2.10) is satisfied.

It remains to find the cycle $\hat{\mathbf{b}}_0$ and this is the most difficult. From (2.10) we see we wish a cycle invariant under σ and having canonical intersections with the other cycles. Such is shown in Figure 6 alongside $\hat{\mathbf{a}}_0$ and their $\alpha = 0$ limits. We record these results as

Theorem 1. *The homology cycles given in figures 5 and 6 are canonical, satisfy (2.10), and have smooth limit $\alpha \rightarrow 0$.*

These cycles can be expanded in terms of “basic arcs” as follows. Denote the arc between the branchpoints \hat{B}_i and \hat{B}_j on sheet k by

$$\gamma_k(i, j) = \text{arc}_k(\hat{B}_i, \hat{B}_j), \quad i \neq j = 1, \dots, 12.$$

Then we have the following

$$(2.12) \quad \begin{aligned} \hat{\mathbf{a}}_1 &= \gamma_1(1, 2) + \gamma_2(2, 1), & \hat{\mathbf{b}}_1 &= \gamma_1(3, 1) + \gamma_2(1, 12) + \gamma_3(12, 3), \\ \hat{\mathbf{a}}_2 &= \gamma_2(5, 6) + \gamma_3(6, 5), & \hat{\mathbf{b}}_2 &= \gamma_2(7, 5) + \gamma_3(5, 4) + \gamma_1(4, 7), \\ \hat{\mathbf{a}}_3 &= \gamma_3(9, 10) + \gamma_1(10, 9), & \hat{\mathbf{b}}_3 &= \gamma_3(11, 9) + \gamma_1(9, 8) + \gamma_2(8, 11), \\ \hat{\mathbf{a}}_0 &= \gamma_1(3, 10) + \gamma_3(10, 9) + \gamma_1(9, 8) + \gamma_2(8, 12) + \gamma_3(12, 3), \\ \hat{\mathbf{b}}_0 &= \gamma_1(2, 8) + \gamma_2(8, 11) + \gamma_3(11, 4) + \gamma_1(4, 7) + \gamma_2(7, 12) + \gamma_3(12, 2). \end{aligned}$$

and, as $\alpha \rightarrow 0$,

$$(2.13) \quad \begin{aligned} \hat{\mathbf{a}}_1^0 &= \gamma_1(1, 2) + \gamma_2(2, 1), & \hat{\mathbf{b}}_1^0 &= \gamma_1(2, 1) + \gamma_3(1, 2), \\ \hat{\mathbf{a}}_2^0 &= \gamma_2(3, 4) + \gamma_3(4, 3), & \hat{\mathbf{b}}_2^0 &= \gamma_2(4, 3) + \gamma_1(3, 4), \\ \hat{\mathbf{a}}_3^0 &= \gamma_3(5, 6) + \gamma_1(6, 5), & \hat{\mathbf{b}}_3^0 &= \gamma_3(6, 5) + \gamma_2(5, 6), \\ \hat{\mathbf{a}}_0^0 &= \gamma_3(1, 2) + \gamma_1(2, 6) + \gamma_3(6, 5) + \gamma_2(5, 1), \\ \hat{\mathbf{b}}_0^0 &= \gamma_3(1, 2) + \gamma_1(2, 5) + \gamma_2(5, 6) + \gamma_3(6, 3) + \gamma_1(3, 4) + \gamma_2(4, 1). \end{aligned}$$

We may complete the specification (2.11) of homology bases by projecting the cycles of Figures 5, 6. The fact that the branchpoints of $\hat{\mathcal{C}}$ do not get mapped by π to branchpoints of \mathcal{C} makes the projection less straightforward². The results are shown in Figure 7. We therefore have a homology basis for the hyperelliptic curve \mathcal{C} differing from standard ones. As we shall see however, the bases chosen allow us to simply relate the period matrices and other quantities of $\hat{\mathcal{C}}$ and \mathcal{C} . With the same notation as above, the arc expansion for these

²This has been implemented in Maple.

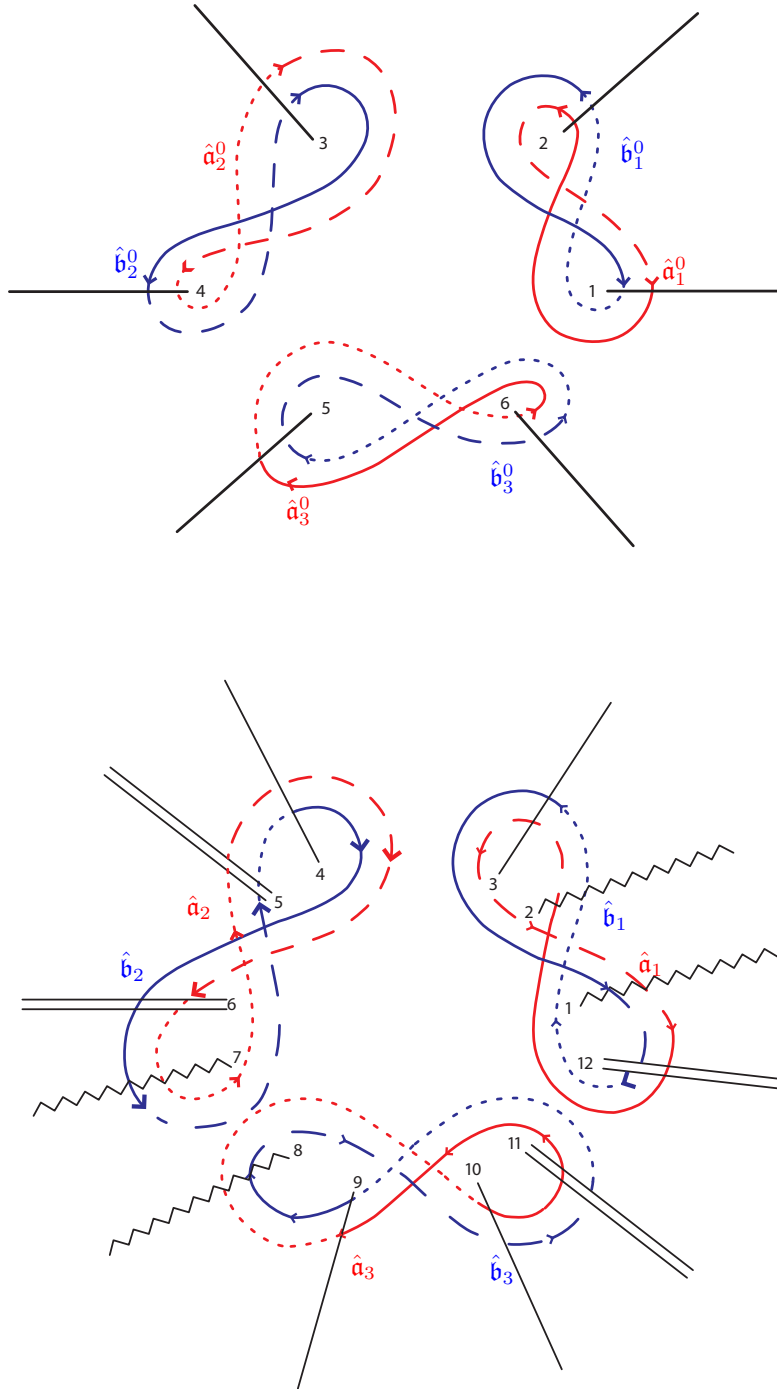


FIGURE 5. Cyclic homology basis

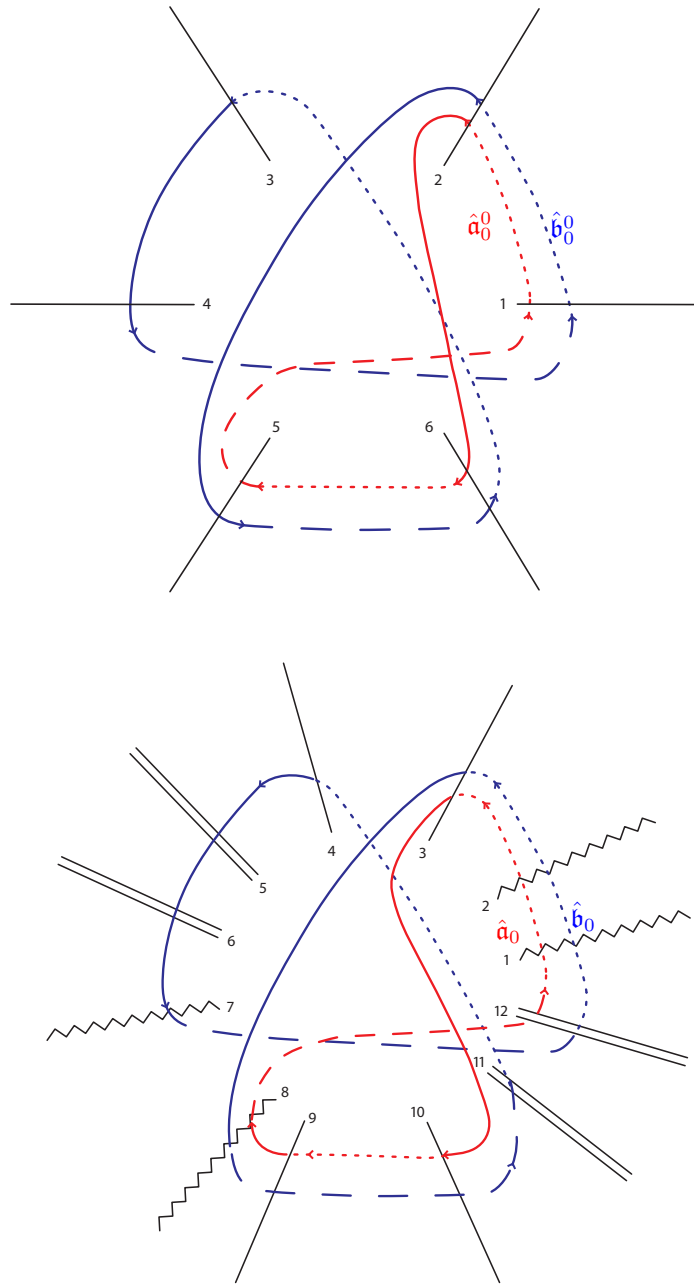
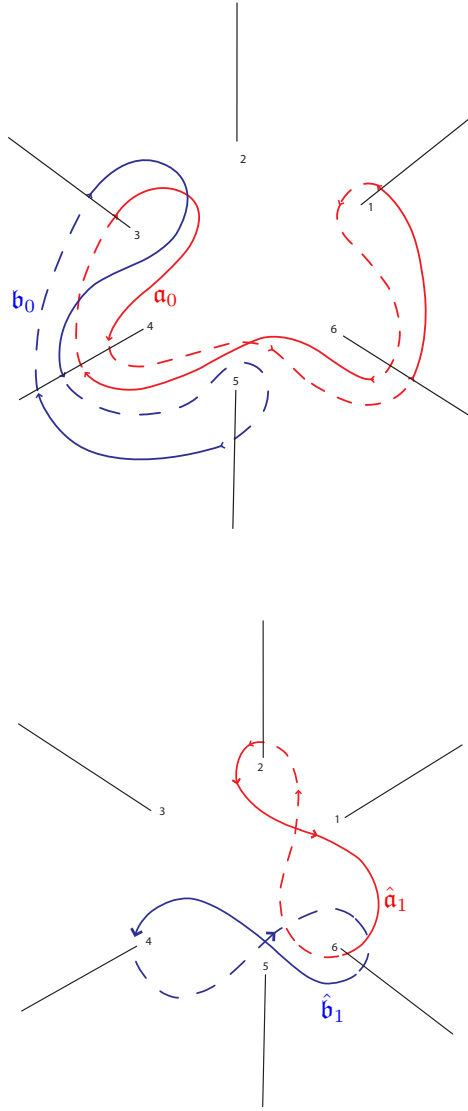


FIGURE 6. Cyclic homology basis

FIGURE 7. Cyclic homology basis for the quotient curve \mathcal{C}

cycles is then

$$\begin{aligned}
 \mathbf{a}_1 &= \gamma_1(2, 6) + \gamma_2(6, 2), \\
 \mathbf{b}_1 &= \gamma_1(6, 4) + \gamma_2(4, 6), \\
 \mathbf{a}_0 &= \gamma_1(3, 4) + \gamma_2(4, 6) + \gamma_1(6, 1) + \gamma_2(1, 6) + \gamma_1(6, 4) + \gamma_2(4, 3), \\
 \mathbf{b}_0 &= \gamma_1(3, 4) + \gamma_2(4, 5) + \gamma_1(5, 4) + \gamma_2(4, 3).
 \end{aligned}
 \tag{2.14}$$

2.4. Period matrices. We shall now relate the period matrices of $\hat{\mathcal{C}}$ and \mathcal{C} and then use the symmetries of $\hat{\mathcal{C}}$ to further restrict the periods involved. If $\{\hat{\mathbf{a}}_\mu, \hat{\mathbf{b}}_\mu\}$ are the canonical homology basis introduced earlier and $\{\hat{\mathbf{u}}_j\}$ any basis of holomorphic differentials for our Riemann surface $\hat{\mathcal{C}}$ we have the matrix of periods

$$(2.15) \quad \begin{pmatrix} \oint_{\hat{\mathbf{a}}_\mu} \hat{\mathbf{u}}_j \\ \oint_{\hat{\mathbf{b}}_\mu} \hat{\mathbf{u}}_j \end{pmatrix} = \begin{pmatrix} \hat{\mathcal{A}} \\ \hat{\mathcal{B}} \end{pmatrix} = \begin{pmatrix} 1 \\ \hat{\tau} \end{pmatrix} \hat{\mathcal{A}}$$

with $\hat{\tau} = \hat{\mathcal{B}}\hat{\mathcal{A}}^{-1}$ the period matrix. The period matrix and periods $\hat{\mathcal{A}}, \hat{\mathcal{B}}$ are our focus here.

To understand the connection between the period matrices $\hat{\tau}$ of $\hat{\mathcal{C}}$ and τ of \mathcal{C} we may first focus on the $\hat{\mathbf{a}}$ -normalized differentials. If $\hat{\mathbf{v}}_i$ are the $\hat{\mathbf{a}}$ -normalized differentials for $\hat{\mathcal{C}}$, then

$$\delta_{i,j+s} = \int_{\hat{\mathbf{a}}_{j+s}} \hat{\mathbf{v}}_i = \int_{\sigma^s(\hat{\mathbf{a}}_j)} \hat{\mathbf{v}}_i = \int_{\hat{\mathbf{a}}_j} (\sigma^s)^* \hat{\mathbf{v}}_i = \int_{\hat{\mathbf{a}}_j} \hat{\mathbf{v}}_{i-s},$$

and we find that

$$(2.16) \quad (\sigma^s)^* \hat{\mathbf{v}}_0 = \hat{\mathbf{v}}_0, \quad (\sigma^s)^* \hat{\mathbf{v}}_i = \hat{\mathbf{v}}_{i-s}.$$

If \mathbf{v}_i are the normalized differentials for \mathcal{C} , then

$$\delta_{ij} = \int_{\mathbf{a}_j} \mathbf{v}_i = \int_{\pi(\hat{\mathbf{a}}_{j+s})} \mathbf{v}_i = \int_{\mathbf{a}_{j+s}} \pi^*(\mathbf{v}_i)$$

shows that

$$\pi^*(\mathbf{v}_i) = \hat{\mathbf{v}}_i + (\sigma)^* \hat{\mathbf{v}}_i + (\sigma^2)^* \hat{\mathbf{v}}_i$$

and similarly that

$$\pi^*(\mathbf{v}_0) = \hat{\mathbf{v}}_0.$$

From (2.16) we have an action of \mathfrak{C}_3 on $\text{Jac}(\hat{\mathcal{C}})$ which lifts to an automorphism of \mathbb{C}^4 by

$$(2.17) \quad \sigma(\hat{z}) = \sigma(\hat{z}_0, \hat{z}_1, \hat{z}_2, \hat{z}_3) = (\hat{z}_0, \hat{z}_3, \hat{z}_2, \hat{z}_1)$$

With the choices above (things are different for $\hat{\mathbf{b}}$ -normalization) we may lift the map $\pi^* : \text{Jac}(\mathcal{C}) \rightarrow \text{Jac}(\hat{\mathcal{C}})$ to $\pi^* : \mathbb{C}^2 \rightarrow \mathbb{C}^4$,

$$\pi^*(z) = \pi^*(z_0, z_1) = (3z_0, z_1, z_1, z_1) = \hat{z}.$$

If we denote points of the Jacobian in characteristic notation by

$$\begin{bmatrix} \alpha \\ \beta \end{bmatrix}_\tau = \alpha\tau + \beta$$

($\alpha, \beta \in \mathbb{R}^2$) then

$$\pi^* \begin{bmatrix} \alpha_0 & \alpha_1 \\ \beta_0 & \beta_1 \end{bmatrix}_\tau = \begin{bmatrix} \alpha_0 & \alpha_1 & \alpha_1 & \alpha_1 \\ 3\beta_0 & \beta_1 & \beta_1 & \beta_1 \end{bmatrix}_{\hat{\tau}}.$$

The period matrices for the two curves are related by [Fay73]

$$(2.18) \quad \hat{\tau} = \begin{pmatrix} a & b & b & b \\ b & c & d & d \\ b & d & c & d \\ b & d & d & c \end{pmatrix}, \quad \tau = \begin{pmatrix} \frac{1}{3}a & b \\ b & c + 2d \end{pmatrix}.$$

The point to note is that although the period matrix for $\hat{\mathcal{C}}$ involves integrations of differentials that do not reduce to hyperelliptic integrals, the combination of terms appearing in the reduction can be expressed in terms of hyperelliptic integrals. This is a definite simplification. Further the Θ function defined by $\hat{\tau}$ has the symmetries

$$\Theta(\hat{z}|\hat{\tau}) = \Theta(\sigma^s(\hat{z})|\hat{\tau})$$

for all $\hat{z} \in \mathbb{C}^4$. In particular, the Θ divisor is fixed under \mathbb{C}_3 .

Now we turn to the symmetries of $\hat{\mathcal{C}}$ to simplify the calculation of periods. If ψ is any automorphism of $\hat{\mathcal{C}}$ then ψ acts on $H_1(\hat{\mathcal{C}}, \mathbb{Z})$ and the holomorphic differentials by

$$\psi_* \begin{pmatrix} \hat{\mathbf{a}}_\mu \\ \hat{\mathbf{b}}_\mu \end{pmatrix} = \begin{pmatrix} A & B \\ C & D \end{pmatrix} \begin{pmatrix} \hat{\mathbf{a}}_\mu \\ \hat{\mathbf{b}}_\mu \end{pmatrix}, \quad \psi^* \hat{\mathbf{u}}_j = \hat{\mathbf{u}}_k L_j^k,$$

where $\begin{pmatrix} A & B \\ C & D \end{pmatrix} \in Sp(8, \mathbb{Z})$ and $L \in GL(4, \mathbb{C})$. Then from

$$\oint_{\psi_* \gamma} \hat{\mathbf{u}} = \oint_\gamma \psi^* \hat{\mathbf{u}}$$

we obtain

$$(2.19) \quad \begin{pmatrix} A & B \\ C & D \end{pmatrix} \begin{pmatrix} \hat{\mathcal{A}} \\ \hat{\mathcal{B}} \end{pmatrix} = \begin{pmatrix} \hat{\mathcal{A}} \\ \hat{\mathcal{B}} \end{pmatrix} L.$$

Thus, for example, from the definition of our homology basis,

$$M_\sigma := \begin{pmatrix} 1 & 0 & 0 & 0 & 0 & 0 & 0 & 0 \\ 0 & 0 & 1 & 0 & 0 & 0 & 0 & 0 \\ 0 & 0 & 0 & 1 & 0 & 0 & 0 & 0 \\ 0 & 1 & 0 & 0 & 0 & 0 & 0 & 0 \\ 0 & 0 & 0 & 0 & 1 & 0 & 0 & 0 \\ 0 & 0 & 0 & 0 & 0 & 0 & 1 & 0 \\ 0 & 0 & 0 & 0 & 0 & 0 & 0 & 1 \\ 0 & 0 & 0 & 0 & 0 & 1 & 0 & 0 \end{pmatrix},$$

while σ acts on the differentials (2.1) as follows

$$(2.20) \quad \sigma^* \hat{\mathbf{u}}_1 = \rho^2 \hat{\mathbf{u}}_1, \quad \sigma^* \hat{\mathbf{u}}_2 = \hat{\mathbf{u}}_2, \quad \sigma^* \hat{\mathbf{u}}_3 = \rho \hat{\mathbf{u}}_3, \quad \sigma^* \hat{\mathbf{u}}_4 = \hat{\mathbf{u}}_4.$$

Let us denote the $\hat{\mathbf{a}}_i$ integrals of $\hat{\mathbf{u}}_1$ by z_i and the corresponding $\hat{\mathbf{b}}_i$ integrals by Z_i ; and similarly those of $\hat{\mathbf{u}}_2$, $\hat{\mathbf{u}}_3$ and $\hat{\mathbf{u}}_4$ by x_i , X_i , w_i , W_i and y_i , Y_i respectively. Then $\hat{\mathcal{A}} = (\mathbf{z}, \mathbf{x}, \mathbf{w}, \mathbf{y})$ (and analogously for $\hat{\mathcal{B}}$). A symmetry relates these various periods. The symmetry σ restricts the matrices of periods to take the following form

$$(2.21) \quad \hat{\mathcal{A}} = \begin{pmatrix} 0 & x_0 & 0 & y_0 \\ z_1 & x_1 & w_1 & y_1 \\ \rho^2 z_1 & x_1 & \rho w_1 & y_1 \\ \rho z_1 & x_1 & \rho^2 w_1 & y_1 \end{pmatrix}, \quad \hat{\mathcal{B}} = \begin{pmatrix} 0 & X_0 & 0 & Y_0 \\ Z_1 & X_1 & W_1 & Y_1 \\ \rho^2 Z_1 & X_1 & \rho W_1 & Y_1 \\ \rho Z_1 & X_1 & \rho^2 W_1 & Y_1 \end{pmatrix}.$$

For instance, we get

$$z_0 = \oint_{\hat{\mathbf{a}}_0} \hat{\mathbf{u}}_1 = \oint_{\sigma(\hat{\mathbf{a}}_0)} \hat{\mathbf{u}}_1 = \oint_{\hat{\mathbf{a}}_0} \sigma^* \hat{\mathbf{u}}_1 = \oint_{\hat{\mathbf{a}}_0} \rho^2 \hat{\mathbf{u}}_1 = \rho^2 z_0,$$

and so $z_0 = 0$, while

$$z_2 = \oint_{\hat{\mathbf{a}}_2} \hat{\mathbf{u}}_1 = \oint_{\sigma(\hat{\mathbf{a}}_0)} \hat{\mathbf{u}}_1 = \oint_{\hat{\mathbf{a}}_0} \sigma^* \hat{\mathbf{u}}_1 = \oint_{\hat{\mathbf{a}}_0} \rho^2 \hat{\mathbf{u}}_1 = \rho^2 z_1,$$

so leading to (2.21).

We now use the other symmetries to further restrict the matrices of periods. The chief difficulty in this approach is in calculating the actions on the homology. In the present

setting we find that

$$(2.22) \quad M_\varphi := \begin{pmatrix} -1 & 0 & 0 & 0 & 0 & 0 & 0 & 0 \\ 0 & 0 & -1 & 0 & 0 & 0 & 0 & 0 \\ 0 & -1 & 0 & 0 & 0 & 0 & 0 & 0 \\ 0 & 0 & 0 & -1 & 0 & 0 & 0 & 0 \\ 0 & 0 & 0 & 0 & -1 & 0 & 0 & 0 \\ 0 & 0 & 0 & 0 & 0 & 0 & -1 & 0 \\ 0 & 0 & 0 & 0 & 0 & -1 & 0 & 0 \\ 0 & 0 & 0 & 0 & 0 & 0 & 0 & -1 \end{pmatrix}, \quad M_\tau := \begin{pmatrix} 2 & 0 & 0 & 0 & 0 & -1 & -1 & -1 \\ 1 & 0 & 1 & 1 & -1 & 0 & 1 & 1 \\ 1 & 1 & 0 & 1 & -1 & 1 & 0 & 1 \\ 1 & 1 & 1 & 0 & -1 & 1 & 1 & 0 \\ 6 & 1 & 1 & 1 & -2 & -1 & -1 & -1 \\ 1 & 0 & 0 & 0 & 0 & 0 & -1 & -1 \\ 1 & 0 & 0 & 0 & 0 & -1 & 0 & -1 \\ 1 & 0 & 0 & 0 & 0 & -1 & -1 & 0 \end{pmatrix},$$

with

$$(2.23) \quad \varphi^* \hat{\mathbf{u}}_1 = \hat{\mathbf{u}}_3, \quad \varphi^* \hat{\mathbf{u}}_2 = -\hat{\mathbf{u}}_2, \quad \varphi^* \hat{\mathbf{u}}_3 = \hat{\mathbf{u}}_1, \quad \varphi^* \hat{\mathbf{u}}_4 = -\hat{\mathbf{u}}_4,$$

$$(2.24) \quad \tau^* \hat{\mathbf{u}}_1 = \overline{\hat{\mathbf{u}}_3}, \quad \tau^* \hat{\mathbf{u}}_2 = -\overline{\hat{\mathbf{u}}_2}, \quad \tau^* \hat{\mathbf{u}}_3 = \overline{\hat{\mathbf{u}}_1}, \quad \tau^* \hat{\mathbf{u}}_4 = -\overline{\hat{\mathbf{u}}_4}.$$

The φ symmetry simplifies the matrices of periods to the form

$$\hat{\mathcal{A}} = \begin{pmatrix} 0 & x_0 & 0 & y_0 \\ z_1 & x_1 & -\rho^2 z_1 & y_1 \\ \rho^2 z_1 & x_1 & -z_1 & y_1 \\ \rho z_1 & x_1 & -\rho z_1 & y_1 \end{pmatrix}, \quad \hat{\mathcal{B}} = \begin{pmatrix} 0 & X_0 & 0 & Y_0 \\ Z_1 & X_1 & -\rho^2 Z_1 & Y_1 \\ \rho^2 Z_1 & X_1 & -Z_1 & Y_1 \\ \rho Z_1 & X_1 & -\rho Z_1 & Y_1 \end{pmatrix}$$

while the real involution relates the entries via

$$(2.25) \quad Z_1 = -(\bar{w}_1 + z_1) = \rho \bar{z}_1 - z_1, \quad W_1 = -(\bar{z}_1 + w_1) = \rho^2 z_1 - \bar{z}_1,$$

$$(2.26) \quad 3X_1 = 2x_0 + \bar{x}_0, \quad 3Y_1 = 2y_0 + \bar{y}_0,$$

$$(2.27) \quad X_0 = 2x_1 + x_0 + \bar{x}_1 + 2X_1, \quad Y_0 = 2y_1 + y_0 + \bar{y}_1 + 2Y_1.$$

Thus all the periods are determined in terms of z_1, x_1, x_0, y_1 and y_0 . Finally there is the bilinear relation

$$0 = x_0 Y_0 - y_0 X_0 + 3(x_1 Y_1 - y_1 X_1).$$

Calculating the period matrix $\hat{\tau} = \hat{\mathcal{B}} \hat{\mathcal{A}}^{-1}$ we obtain the form (2.18) with

$$(2.28) \quad a = \frac{x_1 Y_0 - X_0 y_1}{x_1 y_0 - x_0 y_1}, \quad b = \frac{x_1 Y_1 - X_1 y_1}{x_1 y_0 - x_0 y_1},$$

$$c = \frac{2}{3} \frac{Z_1}{z_1} - \frac{1}{3} \frac{x_0 Y_1 - X_1 y_0}{x_1 y_0 - x_0 y_1}, \quad d = -\frac{1}{3} \frac{Z_1}{z_1} - \frac{1}{3} \frac{x_0 Y_1 - X_1 y_0}{x_1 y_0 - x_0 y_1}.$$

2.4.1. *Weierstrass-Poincaré reduction.* We remark in passing that the symplectic matrix

$$(2.29) \quad T = \begin{pmatrix} 0 & 1 & 1 & 1 & 0 & 0 & 0 & 0 \\ 1 & 0 & 0 & 0 & 0 & 0 & 0 & 0 \\ 0 & 0 & 0 & 0 & 0 & -2 & 1 & 1 \\ 0 & 0 & 1 & -1 & 0 & 0 & 0 & 0 \\ 0 & 0 & 0 & 0 & 0 & 1 & 0 & 0 \\ 0 & 0 & 0 & 0 & 1 & 0 & 0 & 0 \\ 0 & 0 & 0 & -1 & 0 & 0 & 0 & 0 \\ 0 & 0 & 0 & 0 & 0 & -1 & 1 & 0 \end{pmatrix} = \begin{pmatrix} A & B \\ C & D \end{pmatrix}$$

transforms the period matrix (2.18) as

$$\hat{\tau} \rightarrow (C + D\hat{\tau})(A + B\hat{\tau})^{-1} = \begin{pmatrix} -\tau^{c-1} & Q \\ Q^T & \mathfrak{I} \end{pmatrix}$$

where $Q = \text{Diag}(-1/3, 0)$ and

$$\mathfrak{X}' = \begin{pmatrix} \frac{c-d}{6} & \frac{1}{2} \\ \frac{1}{2} & -\frac{1}{2(c-d)} \end{pmatrix}.$$

From this we deduce that

$$(2.30) \quad \text{Im}(c-d) \neq 0.$$

2.4.2. *The antiholomorphic involution for \mathcal{C} .* We have seen that the spectral curve $\hat{\mathcal{C}}$ has real structure (1.2). This real structure is inherited by \mathcal{C} where we have the antiholomorphic involution

$$(2.31) \quad \tau' : (x, y) \mapsto (\bar{x}, -\bar{y}).$$

The effect of this is on the homology above is to reflect in the x -axis and change sheet. Specifically we find that

$$(2.32) \quad M_{\tau'} = \begin{pmatrix} 2 & 0 & 0 & -3 \\ 1 & 2 & -3 & 2 \\ 2 & 1 & -2 & -1 \\ 1 & 0 & 0 & -2 \end{pmatrix}, \quad M_{\tau'}^2 = \text{Id}, \quad M_{\tau'} J M_{\tau'}^T = -J,$$

and where the last identity reflects that $M_{\tau'}$ is antiholomorphic. On the holomorphic differentials we have the simple action

$$\tau'^* \mathbf{u}_1 = -\mathbf{u}_1, \quad \tau'^* \mathbf{u}_2 = -\mathbf{u}_2.$$

2.5. **The Fay-Accola theorem.** Having established homology bases (2.10, 2.11) and the relationship these entail for the corresponding period matrices (2.18) of the curves, we next recall the striking theorem of Fay and Accola applied to our present setting.

Theorem 2 (Fay-Accola). *With respect to the ordered canonical homology bases $\{\hat{\mathbf{a}}_i, \hat{\mathbf{b}}_i\}$ constructed above and for arbitrary $\mathbf{z} = \in \mathbb{C}^2$ we have that*

$$(2.33) \quad \frac{\theta[\hat{e}](\pi^* \mathbf{z}; \hat{\tau})}{\prod_{k=0}^2 \theta \begin{bmatrix} 0 & 0 \\ \frac{k}{3} & 0 \end{bmatrix} (\mathbf{z}; \tau)} = c_0(\hat{\tau})$$

is a non-zero modular constant $c_0(\hat{\tau})$ independent of \mathbf{z} . Here $\hat{\tau}$ and τ are the \mathbf{a} -normalized period matrices for the respective curves given in the above bases and

$$\hat{e} = \pi^*(e) := \pi^* \left(\frac{3-1}{2 \cdot 3}, 0 \right) = (1, 0, 0, 0) \equiv \mathbf{0}.$$

The significance of this theorem is that for flows on the Jacobian of $\hat{\mathcal{C}}$ that arise as pullbacks of flows on the Jacobian of \mathcal{C} we may reduce the theta functions to those of the hyperelliptic spectral curve. We have stated in the introduction that such a connection holds,

$$\lambda \hat{U} - \widetilde{\mathbf{K}} = \pi^*(\lambda U - \mathbf{K}_{\infty_+} + e),$$

and we now describe the quantities appearing in this.

2.6. The vector of Riemann constants. To construct the Baker-Akhiezer function for monopoles there is a distinguished point $\widetilde{\mathbf{K}} \in \text{Jac}(\widehat{\mathcal{C}})$ that Hitchin uses to identify degree $\widehat{g} - 1$ line bundles with $\text{Jac}(\widehat{\mathcal{C}})$. For $n \geq 3$ this point is a singular point of the theta divisor, $\widetilde{\mathbf{K}} \in \Theta_{\text{singular}}$ [BE06]. If we denote the Abel map by

$$\mathcal{A}_{\widehat{Q}}(\widehat{P}) = \int_{\widehat{Q}}^{\widehat{P}} \widehat{u}_i$$

then

$$(2.34) \quad \widetilde{\mathbf{K}} = \widehat{\mathbf{K}}_{\widehat{Q}} + \mathcal{A}_{\widehat{Q}} \left((n-2) \sum_{k=1}^n \widehat{\infty}_k \right).$$

Here $\widehat{\mathbf{K}}_{\widehat{Q}}$ is the vector of Riemann constants for the curve $\widehat{\mathcal{C}}$ and $\widehat{\infty}_k$ are the points above infinity for the curve. If $\mathcal{K}_{\widehat{\mathcal{C}}}$ is the canonical divisor of the curve then $\mathcal{A}_{\widehat{Q}}(\mathcal{K}_{\widehat{\mathcal{C}}}) = -2\widehat{\mathbf{K}}_{\widehat{Q}}$. The righthand side of (2.34) is in fact independent of the base point \widehat{Q} in its definition. Let $\pi(\widehat{\infty}_k) = \infty_+ \in \mathcal{C}$ denote the projection of the points at infinity. Then [Bra10] shows that

$$(2.35) \quad \widetilde{\mathbf{K}} = \pi^*(\mathbf{K}_{\infty_+}) - \widehat{e} = \pi^*(\mathbf{K}_{\infty_+} - e),$$

where the half-period \widehat{e} has been identified in ([Fay73]). Thus we need to calculate the vector of Riemann constants (for the homology bases constructed) for the genus 2 curve (1.5) and where the basepoint for the Abel map is ∞_+ . It will be easier for our calculations to choose one of the branchpoints, say B_1 , and then to obtain the vector of Riemann constants with respect to ∞_+ by using the relation

$$(2.36) \quad \mathbf{K}_{\infty_+} = \mathcal{A}_{\infty_+}(B_1) + \mathbf{K}_{B_1},$$

where \mathcal{A}_{∞_+} is the Abel map with basepoint ∞_+ .

2.6.1. The vector \mathbf{K}_{B_1} . We begin by expressing the integrals over our homology cycles in a simple form as integrals between branch points. Let $\gamma_i(j, k)$ denote the path going from branchpoint B_j to B_k on the cut plane of Figure 4 corresponding to sheet i . With this notation the cycles (2.14) can be expressed as

$$\begin{aligned} \mathbf{a}_1 &= \gamma_1(2, 1) + \gamma_1(1, 6) + \gamma_2(6, 1) + \gamma_2(1, 2), \\ \mathbf{b}_1 &= \gamma_1(6, 5) + \gamma_1(5, 4) + \gamma_2(4, 5) + \gamma_2(5, 6), \\ \mathbf{a}_0 &= \gamma_1(3, 4) + \gamma_2(4, 5) + \gamma_2(5, 6) + \gamma_1(6, 1) + \gamma_2(1, 6) + \gamma_1(6, 5) + \gamma_1(5, 4) + \gamma_2(4, 3), \\ \mathbf{b}_0 &= \gamma_1(3, 4) + \gamma_2(4, 5) + \gamma_1(5, 4) + \gamma_2(4, 3). \end{aligned}$$

These expressions may be further simplified using the hyperelliptic involution $J : (x, y) \rightarrow (x, -y)$, giving $\gamma_{k+1}(2j, 2j+1) = J\gamma_k(2j, 2j+1)$. Also, as the sum of the cycle encircling B_1 and B_2 together with the cycle encircling B_3 and B_4 and the cycle encircling B_5 and B_6 is homologically trivial, we find that relations

$$\int_{\gamma_k(6,5)} \omega = \int_{\gamma_k(1,2)} \omega + \int_{\gamma_k(3,4)} \omega,$$

for any holomorphic differential ω . Similar expressions result from other homologically trivial choices of cycles. These yield

$$\int_{\mathbf{a}_1} \omega = 2 \left(\int_{\gamma_1(2,1)} \omega + \int_{\gamma_1(2,3)} \omega + \int_{\gamma_1(4,5)} \omega \right),$$

$$\begin{aligned}\int_{\mathfrak{b}_1} \omega &= 2 \left(\int_{\gamma_1(1,2)} \omega + \int_{\gamma_1(3,4)} \omega + \int_{\gamma_1(5,4)} \omega \right), \\ \int_{\mathfrak{a}_0} \omega &= 2 \left(\int_{\gamma_1(3,4)} \omega + \int_{\gamma_1(1,2)} \omega + \int_{\gamma_1(3,4)} \omega + \int_{\gamma_1(5,4)} \omega + \int_{\gamma_1(3,2)} \omega + \int_{\gamma_1(5,4)} \omega \right), \\ \int_{\mathfrak{b}_0} \omega &= 2 \left(\int_{\gamma_1(3,4)} \omega + \int_{\gamma_1(5,4)} \omega \right),\end{aligned}$$

and these may be inverted to obtain the integrals between branchpoints. If the ω are taken to be \mathfrak{a} -normalized differentials we have

$$\begin{aligned}\int_{\gamma_1(1,2)} \omega &= \frac{1}{2}(\tau^{(0)} + \tau^{(1)}), & \int_{\gamma_1(2,3)} \omega &= \frac{1}{2}(e^{(0)} + \tau^{(0)} + \tau^{(1)}), & \int_{\gamma_1(3,4)} \omega &= \frac{1}{2}(e^{(0)} + e^{(1)} + \tau^{(0)}), \\ \int_{\gamma_1(4,5)} \omega &= \frac{1}{2}(e^{(0)} + e^{(1)}), & \int_{\gamma_1(5,6)} \omega &= \frac{1}{2}(e^{(0)} + e^{(1)} + \tau^{(1)}),\end{aligned}$$

where $\tau^{(i)}$ and $e^{(i)}$ are the appropriate rows of the period and identity matrices. Thus one can easily deduce the image of each branchpoint under the Abel map (with basepoint B_1). We obtain (together with their characteristic form)

$$\begin{aligned}\mathcal{A}_{B_1}(B_1) = 0 &\equiv \begin{bmatrix} 0 & 0 \\ 0 & 0 \end{bmatrix}, & \mathcal{A}_{B_1}(B_2) = \frac{1}{2}(\tau^{(0)} + \tau^{(1)}) &\equiv \frac{1}{2} \begin{bmatrix} 1 & 1 \\ 0 & 0 \end{bmatrix}, \\ \mathcal{A}_{B_1}(B_3) = \frac{1}{2}e^{(0)} &\equiv \frac{1}{2} \begin{bmatrix} 0 & 0 \\ 1 & 0 \end{bmatrix}, & \mathcal{A}_{B_1}(B_4) = \frac{1}{2}(e^{(1)} + \tau^{(0)}) &\equiv \frac{1}{2} \begin{bmatrix} 1 & 0 \\ 0 & 1 \end{bmatrix}, \\ \mathcal{A}_{B_1}(B_5) = \frac{1}{2}(e^{(0)} + \tau^{(0)}) &\equiv \frac{1}{2} \begin{bmatrix} 1 & 0 \\ 1 & 0 \end{bmatrix}, & \mathcal{A}_{B_1}(B_6) = \frac{1}{2}(e^{(1)} + \tau^{(0)} + \tau^{(1)}) &\equiv \frac{1}{2} \begin{bmatrix} 1 & 1 \\ 0 & 1 \end{bmatrix}.\end{aligned}$$

Following an argument of Farkas and Kra ([FK80] VII.1.2), the vector of Riemann constants takes the form

$$(2.37) \quad \mathbf{K}_{B_1} = -(\mathcal{A}_{B_1}(B_5) + \mathcal{A}_{B_1}(B_6)) = \frac{1}{2}(e^{(0)} + e^{(1)} + \tau^{(1)}) \equiv \frac{1}{2} \begin{bmatrix} 0 & 1 \\ 1 & 1 \end{bmatrix}.$$

2.6.2. *The vector $\mathbf{K}_{\infty+}$.* Once we have calculated the vector of Riemann constants with B_1 as basepoint, we can change its basepoint making use of equation (2.36). One finds

$$(2.38) \quad \mathcal{A}_{\infty+}(B_1) = \frac{2}{3}e^{(1)} + \frac{1}{2}\tau^{(1)} \equiv \begin{bmatrix} \frac{1}{2} & 0 \\ \frac{2}{3} & 0 \end{bmatrix},$$

and consequently

$$(2.39) \quad \mathbf{K}_{\infty+} = \frac{1}{6}e^{(1)} + \frac{1}{2}e^{(2)} + \frac{1}{2}\tau^{(1)} + \frac{1}{2}\tau^{(2)} \equiv \begin{bmatrix} \frac{1}{2} & \frac{1}{2} \\ \frac{1}{6} & \frac{1}{2} \end{bmatrix}.$$

2.6.3. *The case $\alpha = 0$.* In the case where $\alpha = 0$, we have that $3 \int_{\hat{B}_i}^{\hat{B}_j} \in \Lambda$ for any branchpoint, and moreover [BE06] that $\mathcal{A}_{\hat{B}_1} \left(\sum_{k=1}^3 \hat{\omega}_k \right) = 0$. Thus in this case we have

$$\widetilde{\mathbf{K}} = \hat{\mathbf{K}}_{\hat{B}_1} + \mathcal{A}_{\hat{B}_1} \left(\sum_{k=1}^3 \hat{\omega}_k \right) = \hat{\mathbf{K}}_{\hat{B}_1} = \pi^*(\mathbf{K}_{\infty+}) - \hat{e} = \pi^*(\mathbf{K}_{\infty+})$$

which yields

$$\hat{\mathbf{K}}_{\hat{\mathcal{B}}_1} = \pi^*(\mathbf{K}_{\infty+}) = \pi^*\left(\begin{bmatrix} \frac{1}{2} & \frac{1}{2} \\ \frac{1}{6} & \frac{1}{2} \end{bmatrix}\right) = \frac{1}{2} \begin{bmatrix} 1 & 1 & 1 & 1 \\ 1 & 1 & 1 & 1 \end{bmatrix}.$$

This coincides with the result of [BE06] derived by other methods.

3. THE ERCOLANI-SINHA CONDITIONS

Here we shall express the transcendental Ercolani-Sinha constraints on the curve $\hat{\mathcal{C}}$ as conditions on the curve \mathcal{C} and then describe our strategy to solve them.

With the ordering of the differentials (2.1) the Ercolani-Sinha conditions (1.4) take the form

$$(\mathbf{n}, \mathbf{m}) \begin{pmatrix} \hat{\mathcal{A}} \\ \hat{\mathcal{B}} \end{pmatrix} = -2(0, 0, 0, 1),$$

where $\hat{\mathbf{e}}\mathbf{s} = \mathbf{n} \cdot \hat{\mathbf{a}} + \mathbf{m} \cdot \hat{\mathbf{b}}$. Now substituting $(\mathbf{n}, \mathbf{m}) = (n_0, n_1, n_2, n_3, m_0, m_1, m_2, m_3)$ directly into (2.21) and making use of (2.28, 2.30) we may deduce that the Ercolani-Sinha vector takes the form

$$(\mathbf{n}, \mathbf{m}) = (n_0, n, n, n, m_0, m, m, m),$$

and thus $\hat{\mathbf{e}}\mathbf{s}$ is fixed under the spatial symmetry: $\sigma(\hat{\mathbf{e}}\mathbf{s}) = \hat{\mathbf{e}}\mathbf{s}$. (This result was obtained more generally via a different argument in [Bra10].) With this simplification we find the remaining equations encoded in the Ercolani-Sinha conditions take the form

$$(n_0, 3n) \begin{pmatrix} x_0 & y_0 \\ x_1 & y_1 \end{pmatrix} + (m_0, 3m) \begin{pmatrix} X_0 & Y_0 \\ X_1 & Y_1 \end{pmatrix} = -2(0, 1).$$

Now using (2.28) we have that

$$\begin{pmatrix} X_0 & Y_0 \\ X_1 & Y_1 \end{pmatrix} \begin{pmatrix} x_0 & y_0 \\ x_1 & y_1 \end{pmatrix}^{-1} = \begin{pmatrix} 3 & 0 \\ 0 & 1 \end{pmatrix} \begin{pmatrix} a/3 & b \\ b & c+2d \end{pmatrix} = \begin{pmatrix} 3 & 0 \\ 0 & 1 \end{pmatrix} \tau.$$

Upon noting (2.9) and that the periods of $\hat{\mathcal{A}}$ and $\hat{\mathcal{B}}$ were constructed from $\hat{\mathbf{u}}_*$ we obtain

Theorem 3. *The Ercolani-Sinha constraint on the curve $\hat{\mathcal{C}}$ yields the constraint*

$$(3.1) \quad (n_0, 3n, 3m_0, 3m) \begin{pmatrix} \hat{\mathcal{A}} \\ \hat{\mathcal{B}} \end{pmatrix} = -2(0, 1)$$

on the curve \mathcal{C} with respect to the differentials $-dx/(3y)$, $-xdx/(3y)$ and the homology basis $\{\mathbf{a}_0, \mathbf{b}_0, \mathbf{a}_1, \mathbf{b}_1, \}$.

We remark also that we have

$$\hat{\mathbf{U}} = \pi^*(\mathbf{U}), \quad \mathbf{U} = \frac{1}{2}\left(\frac{n_0}{3}, n\right) + \frac{1}{2}(m_0, m)\tau.$$

If we define the cycle

$$(3.2) \quad \mathbf{c} := \pi(\hat{\mathbf{e}}\mathbf{s}) = n_0\mathbf{a}_0 + 3n\mathbf{a}_1 + 3m_0\mathbf{b}_0 + 3m\mathbf{b}_1$$

then the Ercolani-Sinha constraints may be alternately expressed as

$$(3.3) \quad 6\beta_0 = \oint_{\hat{\mathbf{e}}\mathbf{s}} \pi^*(\beta_0\mathbf{u}_2 + \beta_1\mathbf{u}_1) = \oint_{\mathbf{c}} (\beta_0\mathbf{u}_2 + \beta_1\mathbf{u}_1).$$

At this stage then we have reduced the Ercolani-Sinha constraints on the curve $\hat{\mathcal{C}}$ to analogous conditions on the curve \mathcal{C} . We now use the approach outlined in the introduction. We know from [BE06] the values of (\mathbf{n}, \mathbf{m}) of the Ercolani-Sinha vector for the curve (1.6)

for both signs. After changing from the homology basis of that work to that of the present paper we obtain for the two cases of (1.6),

$$(3.4) \quad (n_0, n, m_0, m) = \begin{cases} (4, 1, -3, 1) & +5\sqrt{2}, \\ (5, 1, -3, 0) & -5\sqrt{2}, \end{cases}$$

and so we know the cycle \mathbf{c} for each of the two loci associated to the tetrahedrally symmetric monopoles. We also remark that just as $\tau_*(\widehat{\mathbf{cs}}) = -\widehat{\mathbf{cs}}$ [HMR00] we also have that $\tau'_*(\mathbf{c}) = -\mathbf{c}$. Thus for the $+5\sqrt{2}$ values above and using (2.32) appropriate to this we have $(4, 3, -9, 3)M_{\tau'} = -(4, 3, -9, 3)$ and similarly for $-5\sqrt{2}$ we have $(5, 3, -9, 0)M_{\tau'} = -(5, 3, -9, 0)$.

Now if we now make a change of variable

$$x = \beta^{1/3} X, \quad y = \beta Y, \quad a = \frac{\alpha}{\beta^{2/3}}, \quad g = \frac{\gamma}{\beta}$$

then

$$Y^2 = (X^3 + aX + g)^2 + 4, \quad \mathbf{u}_1 = \frac{dx}{y} = \beta^{-2/3} \frac{dX}{Y}, \quad \mathbf{u}_2 = \frac{x dx}{y} = \beta^{-1/3} \frac{XdX}{Y},$$

and the Ercolani-Sinha constraints take the form

$$(3.5) \quad 0 = \oint_{\mathbf{c}} \frac{dX}{Y},$$

$$(3.6) \quad 6\beta^{1/3} = \oint_{\mathbf{c}} \frac{XdX}{Y}.$$

(We denote by \mathbf{c} the cycle for both the scaled and unscaled curves.) The first of these equations may be viewed as defining $g = g(a)$, and then for this solution the second gives us $\beta = \beta(g)$. Thus solving the Ercolani-Sinha constraints has reduced to determining the relation between g and a given by (3.5). Thus to solve the Ercolani-Sinha constraints we need to be able to compute periods of these hyperelliptic integrals. We shall do this numerically using a variant of the arithmetic-geometric mean used to rapidly and accurately compute periods of elliptic integrals. We shall turn to this in the next section.

4. THE AGM METHOD

In this section we shall recall the connection of the arithmetic-geometric mean (AGM) to evaluating elliptic integrals and Richelot's generalisation of this to the genus two setting. This latter work has been most studied in the setting where the hyperelliptic curve has real branch points and we shall need to extend this discussion to the case with pairs of complex conjugate branch points relevant to the monopole setting.

4.1. AGM: the elliptic case. While the origin of the AGM method dates back to Lagrange it was Gauss who truly initiated its investigation. A large part of what is known today seems to be due (or at least known) to him (for historical notes see *e.g.* [Cox84]). Let $a \geq b$ be positive real numbers. The *arithmetic-geometric mean* of these numbers, denoted $M(a, b)$, is the common limit of the sequences defined as follows:

$$(4.1) \quad \begin{aligned} a_0 &= a, & b_0 &= b, \\ a_{n+1} &= \frac{a_n + b_n}{2}, & b_{n+1} &= \sqrt{a_n b_n}. \end{aligned}$$

These two sequences satisfy

$$a_0 \geq a_1 \geq \dots \geq a_n \geq a_{n+1} \geq \dots \geq b_{n+1} \geq b_n \geq \dots \geq b_1 \geq b_0,$$

which ensures the existence of a common limit

$$\lim_{n \rightarrow \infty} a_n = \lim_{n \rightarrow \infty} b_n = M(a, b).$$

Indeed

$$a_{n+1} - b_{n+1} \leq a_{n+1} - b_n = \frac{1}{2}(a_n - b_n)$$

whence

$$0 \leq a_n - b_n \leq 2^{-n}(a - b),$$

which ensures rapid convergence (which is relevant in the present work).

The remarkable observation of Gauss was the connection of the Arithmetic-Geometric Mean with elliptic integrals.

Theorem 4. AGM [Gau99] *Let $a, b \in \mathbb{R}_+$ and let $M(a, b)$ be their arithmetic geometric mean, then*

$$\int_0^{\pi/2} \frac{d\phi}{\sqrt{a^2 \cos^2 \phi + b^2 \sin^2 \phi}} = \frac{\pi}{2M(a, b)}$$

The theorem may be understood in terms of maps $G_n : \mathcal{E}_n \rightarrow \mathcal{E}_{n+1}$ between the elliptic curves

$$(4.2) \quad \mathcal{E}_n : \quad y_n^2 = x_n(x_n - a_n^2)(x_n - b_n^2).$$

Using Theorem 4 all elliptic integrals of the form $\int_a^b \frac{dx}{\sqrt{P(x)}}$ can be expressed in terms of an appropriate arithmetic geometric mean after various change of variables. We also remark that the restriction $a, b \in \mathbb{R}_+$ may be extended to $a, b \in \mathbb{C}^*$, $a \neq \pm b$, with further discussion of the square roots taken in the geometric mean. We shall not need this extension here.

4.2. Richelot and Humbert: the genus 2 case. Richelot [Ric36, Ric36] extended to the hyperelliptic case Gauss' connection of the AGM with elliptic integrals. Humbert [Hum01] later gave another view of this re-interpreting Richelot's findings in terms of the duplication formulae of 2-variable theta functions, *i.e.* isogenies (of type (2,2)) on Abelian surfaces. We will follow here the modern exposition of Richelot's work given by Bost and Mestre in [BM88] which describes Richelot's "changes of coordinates" in terms of a correspondence (see below).

At the outset we note that the Richelot-Humbert construction is only given for the case where the genus 2 curve (represented as a two-sheeted cover of \mathbb{P}^1 with six branchpoints) has all **real** branchpoints. This manifests itself in what follows by using the ordering of the reals. Just as the AGM of two complex numbers is correspondingly more complicated than the real setting the implementations of the Richelot-Humbert construction do not apply in a straightforward fashion to the case of a genus 2 curve with complex roots. In the next section we describe the generalisation needed to apply this for our monopole curve.

Consider the genus 2 curve \mathcal{C}

$$(4.3) \quad \begin{aligned} & y^2 + P(x)Q(x)R(x) = 0, \\ & P(x) = (x - a)(x - a'), \quad Q(x) = (x - b)(x - b'), \quad R(x) = (x - c)(x - c'), \end{aligned}$$

where the real roots a, a', b, b', c, c' are ordered as

$$a < a' < b < b' < c < c'.$$

We may associate to this triple of (real) polynomials (P, Q, R) another triple, (U, V, W) , defined by

$$(4.4) \quad U(x) = [Q(x), R(x)], \quad V(x) = [R(x), P(x)], \quad W(x) = [P(x), Q(x)].$$

where $[f, g] := \frac{df(x)}{dx}g(x) - \frac{dg(x)}{dx}f(x)$. The roots of the (quadratic) polynomials U, V, W are all real. If we set $u < u', v < v', w < w'$ the roots of U, V, W respectively, then one finds

$$(4.5) \quad a \leq v \leq w \leq a' \leq b \leq w' \leq u \leq b' \leq c \leq u' \leq v' \leq c'.$$

(Explicit expressions for the roots of U, V, W will be given below from which these inequalities can be proven.) Humbert gave a geometric perspective on this construction. Let p_i, p'_i be the roots of (the quadratic) polynomial P_i ($i = 1, 2, 3$). We may view the six branch points $\{p_i, p'_i\} \in \mathbb{P}^1$ as six points on a conic \mathcal{Q} . Now given a conic and six points lying on this we may construct six further points as follows. Consider the lines $L_i := \overline{p_i p'_i}$. The three lines L_i form a triangle and the new points are the points of tangency to \mathcal{Q} from the vertices of this triangle. These are the roots of $[P_1, P_2]$. This is illustrated in Figure 8 below.

We thus have a situation similar to Gauss' AGM case: to each pair of branchpoints one can associate another pair of points which are closer than the initial ones, and we expect a relation between the integrals of corresponding pairs. Iterating this process one shows for every pair the existence of a limit and obtains an expression for the integrals in terms of these limits. The relation between integrals suggested and proven by Humbert is

$$(4.6) \quad \int_a^{a'} \frac{S(x)}{\sqrt{-P(x)Q(x)R(x)}} dx = 2\sqrt{\Delta} \int_v^w \frac{S(x)}{\sqrt{-U(x)V(x)W(x)}} dx,$$

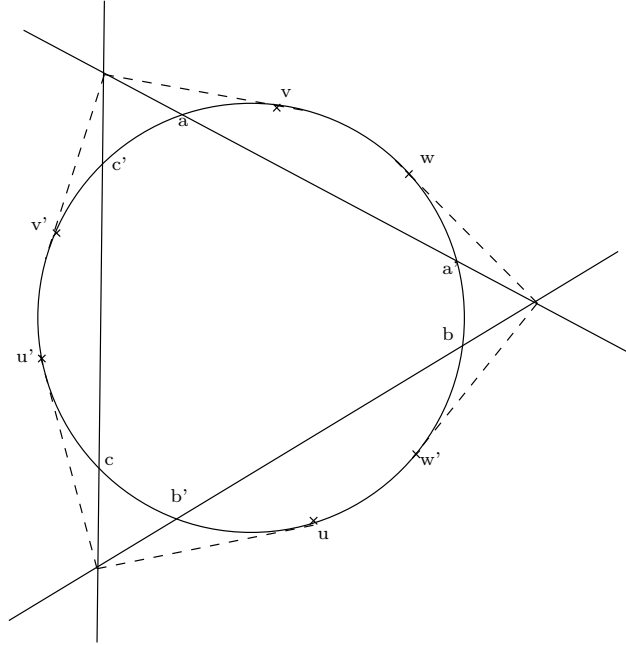


FIGURE 8. Roots of P, Q, R and U, V, W

and similarly for the integrals between the other pairs of branchpoints. Here Δ is the determinant of the matrix whose entries are the coefficients of P, Q, R in the basis $(1, x, x^2)$, and $S(x)$ is a polynomial of degree at most one.

There is, however, an important element of difference between the elliptic and the hyperelliptic cases. The map between elliptic curves (4.2) whose iteration leads to Theorem 4 is replaced by a **correspondence** in the hyperelliptic setting. A correspondence $T : \mathcal{C} \rightarrow \mathcal{C}'$ of degree d between two curves \mathcal{C} and \mathcal{C}' associates to every point $p \in \mathcal{C}$ a divisor $T(p)$ of degree d in \mathcal{C}' , varying holomorphically with p [GH78]. A correspondence can be presented by its “curve of correspondence”, $\mathcal{Z} = \{(p, q) : q \in T(p)\} \subset \mathcal{C} \times \mathcal{C}'$. In the case of the Humbert construction, the two curves are

$$\mathcal{C} : y^2 + P(x)Q(x)R(x) = 0, \quad \mathcal{C}' : \Delta y'^2 + U(x')V(x')W(x') = 0.$$

The correspondence between \mathcal{C} and \mathcal{C}' considered by Humbert [Hum01] is of degree 2, and is given by the curve $\mathcal{Z} \subset \mathcal{C} \times \mathcal{C}'$ of equations

$$(4.7) \quad \begin{cases} P(x)U(x') + Q(x)V(x') = 0, \\ yy' = P(x)U(x')(x - x'). \end{cases}$$

In analogy with the pull-back of a map one can also introduce for correspondences a linear map $\delta_{\mathcal{Z}} : \Omega^1(\mathcal{C}') \rightarrow \Omega^1(\mathcal{C})$. Then eq. (4.6) can be interpreted as the relation between differentials

$$(4.8) \quad \delta_{\mathcal{Z}} \left(\frac{S(x')}{y'} dx' \right) = \frac{S(x)}{y} dx,$$

together with an analysis of the image of the path joining a, a' (resp. b, b' or c, c') under the correspondence. In fact this analysis, while mentioned in passing in [BM88], is rather a crucial point in the extension of Richelot result to the case of complex conjugate roots. Even if one simply integrates on the right hand side along a straight line connecting two branchpoints, the image of this contour via the correspondence (4.7) may be considerably more complicated. Indeed one can obtain nontrivial homology cycles in the image and eq. (4.6) should be interpreted as an identity in $\text{Jac}(\mathcal{C}')$, the Jacobian of \mathcal{C}' . One finds that certain half-periods in \mathcal{C} are sent to periods in \mathcal{C}' via the correspondence.

With this background we may now state a version of the Arithmetic-Geometric Mean for genus 2 curves (with real branch points).

4.2.1. *The AGM method for genus 2 curves.* Consider the genus 2 curve (4.3). Define six sequences $(a_n), (a'_n), (b_n), (b'_n), (c_n), (c'_n)$ recursively by the conditions:

- $a_0 = a, a'_0 = a', b_0 = b, b'_0 = b', c_0 = c, c'_0 = c'$;
- $a_{n+1}, a'_{n+1}, b_{n+1}, b'_{n+1}, c_{n+1}, c'_{n+1}$ are roots of $U_n V_n W_n$, ordered as follows

$$(4.9) \quad a_{n+1} < a'_{n+1} < b_{n+1} < b'_{n+1} < c_{n+1} < c'_{n+1},$$

where, for every n ,

$$\begin{aligned} P_n(x) &= (x - a_n)(x - a'_n), & Q_n(x) &= (x - b_n)(x - b'_n), & R_n(x) &= (x - c_n)(x - c'_n), \\ U_n(x) &= [Q_n(x), R_n(x)], & V_n(x) &= [R_n(x), P_n(x)], & W_n(x) &= [P_n(x), Q_n(x)]. \end{aligned}$$

Bost and Mestre [BM88] give an explicit expression for these sequences:

$$(4.10) \quad \begin{aligned} a_{n+1} &= \frac{c_n c'_n - a_n a'_n - B_n}{c_n + c'_n - a_n - a'_n}, & a'_{n+1} &= \frac{b_n b'_n - a_n a'_n - C_n}{b_n + b'_n - a_n - a'_n}, \\ b_{n+1} &= \frac{b_n b'_n - a_n a'_n + C_n}{b_n + b'_n - a_n - a'_n}, & b'_{n+1} &= \frac{c_n c'_n - b_n b'_n - A_n}{c_n + c'_n - b_n - b'_n}, \\ c_{n+1} &= \frac{c_n c'_n - b_n b'_n + A_n}{c_n + c'_n - b_n - b'_n}, & c'_{n+1} &= \frac{c_n c'_n - a_n a'_n + B_n}{c_n + c'_n - a_n - a'_n}, \end{aligned}$$

with

$$\begin{aligned} A_n &= \sqrt{(b_n - c_n)(b_n - c'_n)(b'_n - c_n)(b'_n - c'_n)}, \\ B_n &= \sqrt{(c_n - a_n)(c_n - a'_n)(c'_n - a_n)(c'_n - a'_n)}, \\ C_n &= \sqrt{(a_n - b_n)(a_n - b'_n)(a'_n - b_n)(a'_n - b'_n)}. \end{aligned}$$

These can be derived finding the roots for U_n, V_n, W_n as follows

$$(4.11) \quad \begin{aligned} u_n, u'_n &= \frac{c_n c'_n - b_n b'_n \mp A_n}{c_n + c'_n - b_n - b'_n}, \\ v_n, v'_n &= \frac{c_n c'_n - a_n a'_n \mp B_n}{c_n + c'_n - a_n - a'_n}, \\ w_n, w'_n &= \frac{b_n b'_n - a_n a'_n \mp C_n}{b_n + b'_n - a_n - a'_n}, \end{aligned}$$

and ordering them according to (4.9). One sees directly from the expressions above that $v_n \leq w_n \leq w'_n \leq u_n \leq u'_n \leq v'_n$ (cf. also eq. (4.5)). Thus we set

$$(4.12) \quad a_{n+1} = v_n, \quad a'_{n+1} = w_n, \quad b_{n+1} = w'_n, \quad b'_{n+1} = u_n, \quad c_{n+1} = u'_n, \quad c'_{n+1} = v'_n,$$

and (4.10) then follow. We then obtain:

Theorem 5 (*Richelot* [Ric36], *Bost and Mestre* [BM88]). *With the above definitions, the sequences $(a_n), (a'_n), (b_n), (b'_n), (c_n), (c'_n)$ converge pairwise to common limits*

$$\begin{aligned} \lim_{n \rightarrow \infty} a_n &= \lim_{n \rightarrow \infty} a'_n = \alpha \equiv M(a, a'), \\ \lim_{n \rightarrow \infty} b_n &= \lim_{n \rightarrow \infty} b'_n = \beta \equiv M(b, b'), \\ \lim_{n \rightarrow \infty} c_n &= \lim_{n \rightarrow \infty} c'_n = \gamma \equiv M(c, c'). \end{aligned}$$

Furthermore, for any polynomial $S(x)$ of degree at most one, the following relations hold:

$$(4.13) \quad \begin{aligned} I(a, a') &\equiv \int_a^{a'} \frac{S(x) dx}{\sqrt{-P(x)Q(x)R(x)}} = \pi T \frac{S(\alpha)}{(\alpha - \beta)(\alpha - \gamma)}, \\ I(b, b') &\equiv \int_b^{b'} \frac{S(x) dx}{\sqrt{-P(x)Q(x)R(x)}} = \pi T \frac{S(\beta)}{(\beta - \alpha)(\beta - \gamma)}, \\ I(c, c') &\equiv \int_c^{c'} \frac{S(x) dx}{\sqrt{-P(x)Q(x)R(x)}} = \pi T \frac{S(\gamma)}{(\gamma - \alpha)(\gamma - \beta)}, \end{aligned}$$

where

$$(4.14) \quad T = \prod_{n=0}^{\infty} t_n, \quad t_n = \frac{2\sqrt{\Delta_n}}{\sqrt{(b_n + b'_n - a_n - a'_n)(c_n + c'_n - b_n - b'_n)(c_n + c'_n - a_n - a'_n)}}.$$

The proof of the convergence of the sequences (a_n) , (a'_n) (and likewise (b_n) , (b'_n) ; (c_n) , (c'_n)) is similar to that of the elliptic case. Using (4.6) we find

$$(4.15) \quad \int_{a_n}^{a'_n} \frac{S(x)}{\sqrt{-P_n Q_n R_n}} dx = 2\sqrt{\Delta_n} \int_{a_{n+1}}^{a'_{n+1}} \frac{S(x)}{\sqrt{-[P_n, Q_n][Q_n, R_n][R_n, P_n]}} dx \\ = t_n \int_{a_{n+1}}^{a'_{n+1}} \frac{S(x)}{\sqrt{-P_{n+1} Q_{n+1} R_{n+1}}} dx,$$

and the relations (4.13) follow upon taking the limit for $n \rightarrow \infty$ and using the residue theorem. Integrals between other pairs of branchpoints (*e.g.* a' and b) may also be calculated using the same method in conjunction with appropriate fractional linear transformations. We remark that the integral between b and b' given above has opposite sign to that in [BM88], because of a different choice of conventions³.

4.3. Generalisation to the genus 2 case with complex conjugate roots. We now generalise Richelot's method of the previous section to the case where the branchpoints are not all real but the polynomials P, Q, R are still real. This corresponds to the three pairs of complex conjugate branchpoints,

$$a' = \bar{a}, \quad b' = \bar{b}, \quad c' = \bar{c},$$

the case relevant for our monopole curve (1.5). We further order the roots such that

$$\operatorname{Re}(a) = \operatorname{Re}(a') < \operatorname{Re}(b) = \operatorname{Re}(b') < \operatorname{Re}(c) = \operatorname{Re}(c')$$

and for definiteness take $\operatorname{Im}(a) < 0$, $\operatorname{Im}(b) < 0$, $\operatorname{Im}(c) < 0$. This splitting into complex conjugate pairs was given for the quotient monopole curve in (2.6) and (2.7).

Of course all of the polynomial relations given in the previous sections extend to the case of arbitrary complex branchpoints and so the relation (4.8) between the differentials on \mathcal{C} and \mathcal{C}' still holds true for this case. The difference with complex branch points arises at two points. First, with complex roots, there is no natural way to order the branchpoints and hence no natural way of splitting the branchpoints into pairs; thus there is choice in constructing a sequence of branchpoints to iterate. (This same feature is present with the ordinary AGM when the elliptic curve does not have real structure.) Second, as noted earlier, the image of the path between branchpoints under the correspondence may be quite complicated. Restricting attention to the case of the three quadratics P, Q, R having complex conjugate roots simplifies the problem somewhat. Although the initial branchpoints are complex and a relation analogous to (4.5) cannot be written, nevertheless the roots of U_0, V_0, W_0 are real (as can be seen by considering their explicit expressions in (4.11)) and so can be ordered. In contrast with the purely real case however, this ordering is not unique: in the real case the ordering of u, u', v, v', w, w' depended only on the relative ordering of a, a', b, b', c, c' on the real line; in the complex conjugate case this now depends on their imaginary parts. Depending on the ordering of u, u', v, v', w, w' , equation (4.15) relating the integrals between the three pairs of branchpoints on \mathcal{C} and \mathcal{C}' needs to be modified appropriately. We shall focus here on the case relevant for the monopole quotient curve.

³Bost and Mestre, in their note 2, p. 51 of [BM88], claim that they want to recover the ‘‘classical identity’’ $I_a - I_b + I_c = 0$. With our choice of convention for sheets, the relation between integrals become $I_a + I_b + I_c = 0$, which follows from the fact that the integral around a cycle encircling all the cuts, oriented so that the upper arc goes from negative to positive real values, is zero.

4.3.1. *The AGM method for the quotient monopole curve.* Consider the quotient monopole curve (1.5). Ordering the branchpoints as in section 2.1 we have

$$(4.16) \quad a = B_4, \quad a' = B_3; \quad b = B_5, \quad b' = B_2; \quad c = B_6, \quad c' = B_1.$$

Calculating u, u', v, v', w, w' via (4.11), and examining their relative ordering we find the following two cases:

$$(4.17) \quad \text{case 1 : } \alpha > 0, \quad v \leq w \leq w' \leq u \leq u' \leq v';$$

$$(4.18) \quad \text{case 2 : } \alpha < 0, \quad u \leq v \leq w \leq u' \leq v' \leq w'.$$

Case 1. This is exactly the same situation as considered in [BM88], Thus (4.12) still holds and so the sequences $a_n, a'_n, b_n, b'_n, c_n, c'_n$ are still given by (4.10). Therefore the first equality in (4.15) holds in view of (4.17) and so the integrals between complex conjugate pairs of branchpoints are still expressed by (4.13). We shall return to a discussion of integrals between other pairs of branchpoints shortly.

Case 2. The different ordering of (4.18) means that (4.12) no longer holds for the first step of the recurrence. We modify this as follows. In view of (4.18) for $n = 1$ we take

$$a_1 = u, \quad a'_1 = v, \quad b_1 = w \quad b'_1 = u', \quad c_1 = v', \quad c'_1 = w'.$$

Now at this stage the curve \mathcal{C}' has all real branchpoints and hence the Richelot-Humbert iteration can be applied as previously. Thus the only change in this case occurs at the first step of the recurrence. Let us denote by $I(p, q)$ the integral on \mathcal{C} between p, q on the first sheet, and by $I^{(i)}$ the integrals on the curve $\mathcal{C}^{(i)}$ of equation $y^2 + P_i(x)Q_i(x)R_i(x) = 0$ on the same sheet. The integrals $I^{(i)}$ can be then expressed by equations (4.13), using the AGM method for the curve $\mathcal{C}^{(1)}$. We obtain an expression for the integrals $I(p, q)$ on \mathcal{C} as follows. Numerically⁴ we calculate the images on \mathcal{C}' under the correspondence (4.7) of the straight line contours of integration between the branchpoints of \mathcal{C} . The resulting contours of integration on the right hand side of (4.19) yield

$$(4.19) \quad \begin{aligned} I(a, a') &= t_0 I'(a'_1, b_1), \\ I(b, b') &= t_0 I'(c'_1, a_1) = t_0 (-I'(a'_1, b_1) + I'(b'_1, c_1)), \\ I(c, c') &= -t_0 I'(b'_1, c_1). \end{aligned}$$

A similar numerical analysis of the images of the paths between other pairs of branchpoints then yields

$$(4.20) \quad \begin{aligned} I(a, b) &= \frac{1}{2} t_0 (I'(a_1, a'_1) + I'(b'_1, c_1)), \\ I(a', b') &= \frac{1}{2} t_0 (I'(a_1, a'_1) - I'(b'_1, c_1)), \\ I(b, c) &= \frac{1}{2} t_0 (-I'(a_1, a'_1) + I'(a'_1, b_1) - I'(b_1, b'_1)), \\ I(b', c') &= \frac{1}{2} t_0 (-I'(a_1, a'_1) - I'(a'_1, b_1) - I'(b_1, b'_1)). \end{aligned}$$

⁴More specifically, we study the images on the curve \mathcal{C}' of equation $\Delta y^2 + U(x)V(x)W(x) = 0$, in order to understand the first equality of (4.15) (as the second follows immediately from the first). We find, for instance, that the straight line between a and a' on \mathcal{C} , call it $\gamma(a, a')$, is sent to a closed cycle encircling a'_1 and b_1 on \mathcal{C}' . Noticing that in the second equality of (4.15) there is a factor of $1/2$, absorbed in the definition of t_i , we obtain that the image of $\gamma(a, a')$ on the curve $y^2 + P_1(x)Q_1(x)R_1(x) = 0$, *i.e.* \mathcal{C}' , is precisely the path from a'_1 and b_1 .

Recalling that we are able to express the integrals $I'(p, q)$ applying the AGM method to the curve \mathcal{C}' (with real branchpoints) using Theorem 5 and earlier remarks we are able then to calculate all integrals between branchpoints on \mathcal{C} .

Finally, we can apply similar numerical considerations to the integrals between non complex conjugate branchpoints in **case 1** to obtain

$$\begin{aligned}
 I(a, a') &= t_0 I'(a_1, a'_1), \\
 I(b, b') &= t_0 I'(b_1, b'_1), \\
 I(c, c') &= t_0 I'(c_1, c'_1), \\
 I(a, b) &= \frac{1}{2} t_0 (I'(a'_1, b_1) - I'(c_1, c'_1)), \\
 I(a', b') &= \frac{1}{2} t_0 (I'(a'_1, b_1) + I'(c_1, c'_1)), \\
 I(b, c) &= \frac{1}{2} t_0 (-I'(b_1, b'_1) - I'(b'_1, c_1) - I'(c_1, c'_1)), \\
 I(b', c') &= \frac{1}{2} t_0 (I'(b_1, b'_1) + I'(b'_1, c_1) + I'(c_1, c'_1)).
 \end{aligned}
 \tag{4.21}$$

5. SOLVING THE ERCOLANI-SINHA CONSTRAINTS VIA THE AGM

We have shown how the Ercolani-Sinha constraints are reduced to finding the $(a, g) := (\alpha/\beta^{2/3}, \gamma/\beta)$ such

$$0 = \oint_{\mathbf{c}} \frac{dX}{Y}, \quad Y^2 = (X^3 + aX + g)^2 + 4
 \tag{5.1}$$

and for the cycle \mathbf{c} given by (3.2) and (3.4) for $a > 0$ and $a < 0$. Our strategy is as follows. Using the arc expansion (2.14) we may express the cycle \mathbf{c} in terms of integrals between branchpoints. These integrals are then evaluated via the AGM method of the previous section using (4.13, 4.21) for the case $a > 0$ and (4.19, 4.19) for $a < 0$. This has been implemented in Maple. The advantage of the AGM method is that it is much faster than the direct numerical integrations between branchpoints as it deals only with polynomial manipulations; moreover, the convergence of the sequences (a_n) , (a'_n) , (b_n) , (b'_n) , (c_n) only needs very few steps, usually 6 or 7, for the precision we require. These considerations allow us to successfully solve the Ercolani-Sinha constraints iteratively, as described in the next subsection. A useful check of the method is the calculation of the matrix of \mathbf{a} and \mathbf{b} periods. These periods may again be reduced to integrals between branchpoints using the arc expansion (2.14) and consequently evaluated via the AGM. We find agreement with the same quantities being evaluated by other methods, yet with significant improvement in speed.

5.1. Numerical solutions. To begin, we wish to find solutions to (5.1) starting from the point $a = 0$ and $g = 5\sqrt{2}$. The integral over \mathbf{c} is reduced to integrals between branchpoints as described above. We then proceed iteratively as follows. We start varying α by a small ϵ , namely $\alpha_i = i \cdot \epsilon$; we then vary γ in smaller steps, $\gamma_{i,k} = 5\sqrt{2} + k \cdot \epsilon^2$. For every such pair $(\alpha_i, \gamma_{i,k})$ we calculate the periods using the AGM method, and hence compute the first constraint in (5.1). For every α_i we take the $\gamma_{i,k}$ for which this constraint vanishes. We repeat this a sufficiently large number of times, obtaining the curve in Figure 9. We have used a step size of 10^{-1} for $a \in (0, 2.8)$, and of 10^{-2} for $a \in (2.8, 3.0)$ to obtain greater detail in this interval. For values of $a \in (0, 3)$, the outcome is that we have a curve of

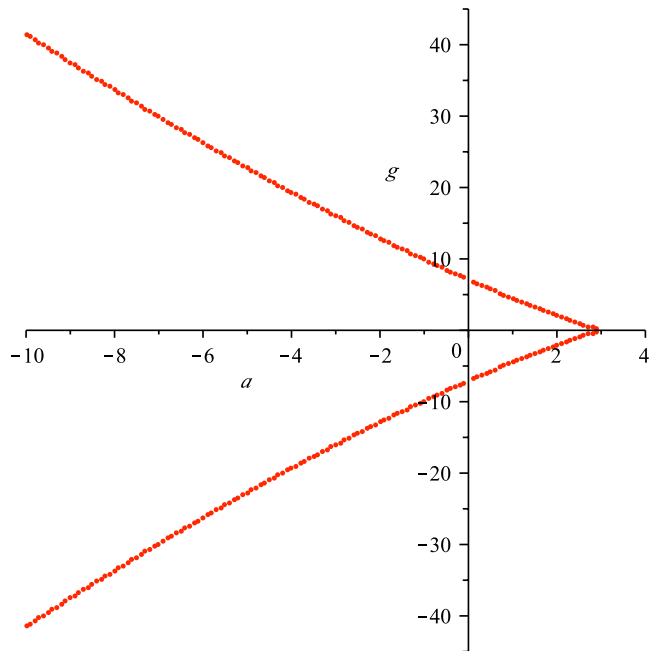


FIGURE 9. Solutions to the Ercolani-Sinha constraints

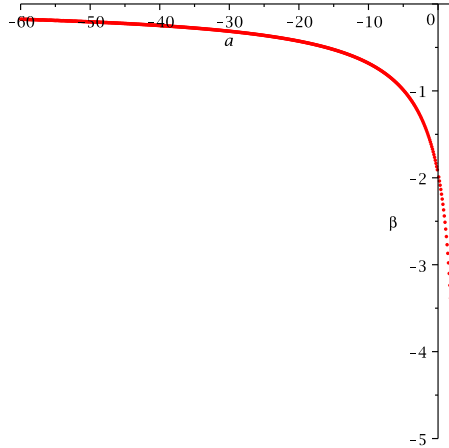
solutions in the space of parameters passing through the points $(0, 5\sqrt{2})$ up to the point $(3, 0)$. This point does not however belong to the solution curve. We may also extend this curve for negative values of a to the left of the point $(0, 5\sqrt{2})$. In Figure 9 we plot 100 points corresponding to $a < 0, g > 0$.

The point $(a, g) = (3, 0)$ is in fact a singular point as 4 of the branchpoints collide pairwise, giving two singular points at $\pm i$. This results in a rational curve with equation

$$(5.2) \quad y^2 = (x^3 + 3x)^2 + 4 = (x^2 + 4)(x^2 + 1)^2.$$

Note that the curves of equation (5.1) with $g = 0$ and $a > 0$ are all hyperelliptic with the only exception being precisely the case $a = 3$ above where the curve is reducible. In terms of the original spectral curve (1.3) we have $\alpha^3 = 27\beta^2$ and [HMM95] noted the loci under consideration here being asymptotic to this at one end. As a rational curve has no nontrivial cycles, the second of the Ercolani-Sinha constraints (3.6) that fixes β tells us $\beta = \infty$ and so our solution curves are asymptotic to the point $(a, g) = (3, 0)$. We remark that the behaviour of the solution curve in Figure 9 is consistent with the findings of [Sut97], where Sutcliffe predicts that the curve (5.2), describing a configurations of three unit-charge monopoles with dihedral D_3 symmetry, constitutes an asymptotic state for a 3-monopole configuration (cf. eq. (4.16) in [Sut97]).

When trying to extend the solution curve to $g < 0$, we do not observe any values of the parameters satisfying (5.1) with the first set of integers of (3.4). But since the point $(a, g) = (3, 0)$ does not belong to the solution curve, continuity arguments do not prevent us using the second set of integers of (3.4). With these we manage to extend the solution curve through the point $(0, -5\sqrt{2})$, which again corresponds to a tetrahedral monopole, now with a different orientation. This curve is also shown in Figure 9 We point out that the arc of the

FIGURE 10. $\beta = \beta(a)$

curve for $g < 0$ is precisely the reflection with respect to the a -axis of the arc obtained for $g > 0$. Because of this symmetry we may focus attention on the case $g > 0$ in what follows.

Having determined the relationship between a and g we then use this to find β via

$$6\beta^{1/3} = \oint_{\mathfrak{c}} \frac{XdX}{Y}.$$

Again these are just integrals determined via the AGM and we present $\beta = \beta(a)$ in Figure 10. We shall interpret these results and compare them with other work in the next section.

6. DISCUSSION

Before discussing our results let us summarise our argument thus far. In this paper we have constructed the spectral curve associated to charge three monopoles with cyclic (but not dihedral) symmetry C_3 . By imposing cyclic symmetry the original genus 4 spectral curve $\hat{\mathcal{C}}$ (1.3) was shown to cover the genus two hyperelliptic curve \mathcal{C} (1.5). By making use of a well adapted homology basis, the theta functions and data appropriate for the monopole solution were shown to be expressible in terms analogous data for the quotient curve \mathcal{C} . Thus the construction of an appropriate spectral curve reduced to questions purely in terms of the curve \mathcal{C} . In particular the transcendental constraints of the Hitchin construction reduce to the single transcendental constraint

$$0 = \oint_{\mathfrak{c}} \frac{dX}{Y}$$

for the scaled curve $Y^2 = (X^3 + aX + g)^2 + 4$ and a specified cycle \mathbf{c} . This may be viewed as defining a function $g = g(a)$ and the monopole curve is determined in terms of this. The “special function” $g(a)$ warrants further study. Here we have made a numerical study of this. Our numerical study used a genus 2 extension of the arithmetic-geometric mean found by Richelot. Like its genus one counterpart Richelot’s extension converges extremely rapidly and is an excellent means of evaluating such integrals. Richelot’s method has (to our understanding) been used almost entirely in the setting of genus two curves with real branch points. When extended to the case of complex (here conjugate) branch points several new features arose.

Our results extend work of both Hitchin, Manton and Murray [HMM95] and Sutcliffe [Sut97] which both describe cyclically symmetric charge three monopoles. In the former the following picture of the scattering of three monopoles, corresponding to geodesic motion along one of our loci is given. Three unit charge monopoles come in at the vertices of an equilateral triangle, moving towards its centre, in the $x_1 - x_2$ plane. Asymptotically this equilateral triangular configuration corresponds to the reducible spectral curve at $a = 3$. At $a = 0$ the three monopoles coalesce instantaneously into a tetrahedron. Depending on whether the equilateral triangle is below or above the $x_1 - x_2$ plane we have distinct orientations of the tetrahedron corresponding to $g > 0$ or $g < 0$. Finally the tetrahedron (with say $g > 0$) breaks up into a unit charge monopole moving along the positive x_3 -axis at $(0, 0, b)$ and an axisymmetric charge 2 monopole, moving along the negative x_3 -axis at $(0, 0, -b/2)$. The reducible curve corresponding to the product of these configurations is

$$0 = (\eta + 2b\zeta)(\eta^2 - 2b\eta\zeta + [b^2 + \frac{\pi^2}{4}]\zeta^2) = \eta^3 + [\frac{\pi^2}{4} - 3b^2]\eta\zeta^2 + 2b(b^2 + \frac{\pi^2}{4})\zeta^3$$

from which we have the asymptotic behaviour at this end of the scattering given by

$$(6.1) \quad \alpha \sim (\pi^2/4 - 3b^2), \quad \gamma \sim 2b(b^2 + \pi^2/4), \quad \beta \sim 0,$$

where we have ignored terms vanishing as b tends to infinity. Sutcliffe investigated the same locus of monopoles numerically finding approximate twistor data by considering Painlevé analysis of the Nahm data at the pole. This led to approximate forms of α , β and γ described parametrically. In Figures 11, 12 we plot this approximate data alongside the exact results. Despite not actually giving a spectral curve at any point the energy densities obtained by Sutcliffe upon solving the Nahm equations qualitatively reflect the scattering behaviour described above. To compare with the asymptotic prediction (6.1) we must revert to α and γ . In Figure 13 we give a log-log plot of the exact values against this asymptotic prediction and alongside that of Sutcliffe’s approximate curve. Our results reproduce the asymptotic behaviour of (6.1). In fact our approach could be extended to enable the calculation of both analytic and numerical corrections to this leading behaviour.

There exists a rather nontrivial check of our results. We have argued that the Hitchin constraint **H3** is automatically satisfied by our construction. This means that each of the three theta functions $\theta \begin{bmatrix} 0 & 0 \\ k & 0 \\ \frac{k}{3} & 0 \end{bmatrix} (z; \tau)$ of (2.33) (with $k = 0, 1, 2$) should be nonvanishing for $\lambda \in (0, 2)$ and two of the three should vanish at the endpoints. A sample check is shown in Figure 14 for $a = -12.3$, with Figure 15 showing an enlarged portion of the $k = 0$ curves to confirm the nonvanishing. Such a numerical plot is the only means we know of for verifying this condition.

Although our construction is generically in terms of a genus two curve it may happen that this curve covers an elliptic curve. Such occurs for the tetrahedral monopole. Shaska and Völklein [SV04] describe when genus two curves give 2 : 1 covers of elliptic curves. For

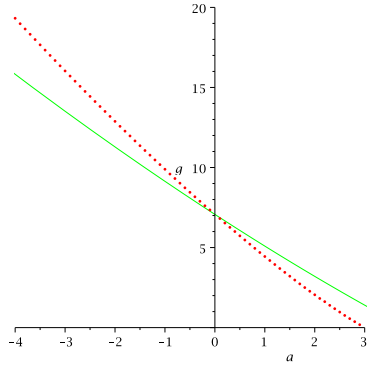


FIGURE 11. $g(a)$ for small values compared with Sutcliffe's approximation (solid line).

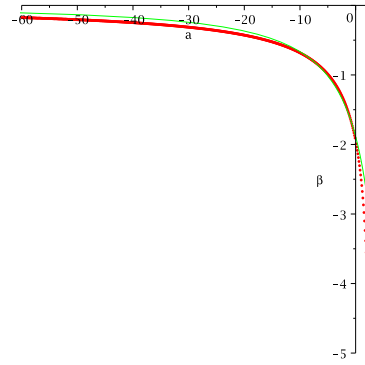


FIGURE 12. $\beta(a)$ compared with Sutcliffe's approximation (solid line).

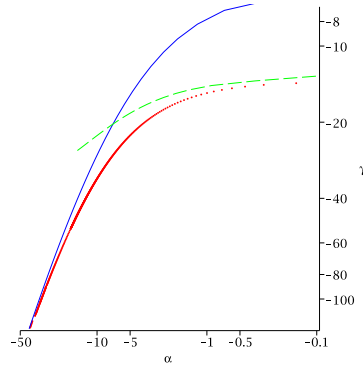


FIGURE 13. A log-log plot of the asymptotic behaviour of α versus γ according to Hitchin, Manton and Murray (solid), Sutcliffe (dash) and here (dots).

our curves these correspond to the axes $a = 0$ (D_3 symmetric monopoles) and $g = 0$ and also to the solid line given in Figure 16. We see that our curve covers an elliptic curve at two further points for $0 < a < 3$ and $g > 0$ (and similarly for $g < 0$). These points do not appear to be otherwise special. For example, Sutcliffe studies the zeros of the Higgs field

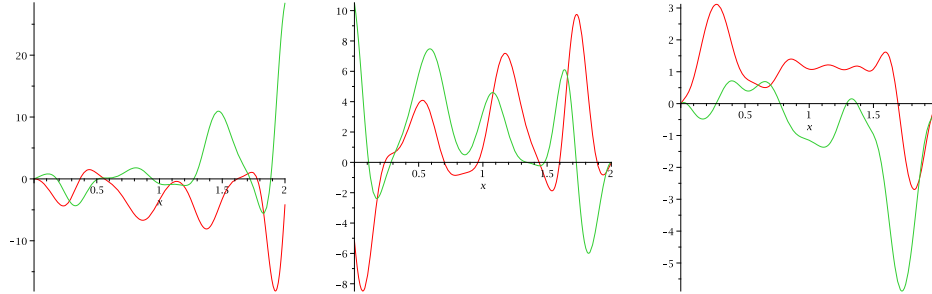


FIGURE 14. A plot of the real and imaginary parts of the genus two theta functions (2.33) for $k = 0, 1, 2$.

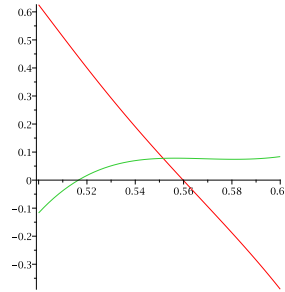


FIGURE 15. An enlargement of the $k = 0$ behaviour showing nonvanishing.

and shows there is a point of positive a for which there is a ‘zero anti-zero’ creation event [Sut97]; both our points are different from Sutcliffe’s.

ACKNOWLEDGEMENTS

We wish to thank T.P Northover for many fruitful discussions. His programs `cyclepainter` and `extcurves` have been used at many stages in this work.⁵

A. D. is grateful for a Small Project Grant (#3606) of the University of Edinburgh which partially funded a visit to Kiev where part of this work was developed. VZE is grateful to Hanse-Wissenschaftskolleg (Institute for Advanced Study), Delmenhorst, for a fellowship during which time the final version of this paper was completed.

⁵These are available from <http://gitorious.org/riemanncycles>.

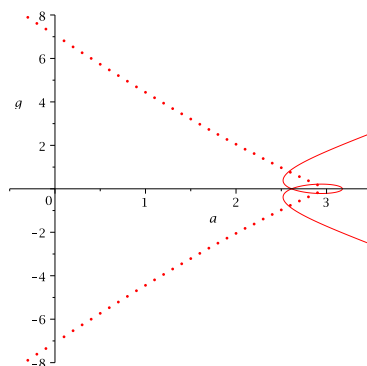


FIGURE 16. The Genus 2 curve covering elliptic curves

REFERENCES

- [AF06] Abenda S., Fedorov, Yu. N. *Closed geodesics and billiards on quadrics related to elliptic KdV solutions*, Lett. Math. Phys. **76** 111-134 (2006). [arXiv:nlin/0412034](#).
- [Acc71] Robert D. M. Accola, *Vanishing Properties of Theta Functions for Abelian Covers of Riemann Surfaces*, p7-18 in *Advances in the Theory of Riemann Surfaces: Proceedings of the 1969 Sony Brook Conference*, edited by L.V. Ahlfors, L. Bers, H.M. Farkas, R.C. Gunning, I. Kra and H.E. Rauch (Princeton University Press 1971).
- [BE06] H. W. Braden and V. Z. Enolski, *Remarks on the complex geometry of 3-monopole*, arXiv: math-ph/0601040, 2006.
- [BE09A] ———, *Finite-gap integration of the SU(2) Bogomolny equations*, Glasgow Math.J. **51** (2009) 25–41. arXiv: [math-ph/0806.1807](#)
- [BE09B] ———, *On the tetrahedrally symmetric monopole*, To appear Commun. Math. Phys. arXiv: [math-ph/0908.3449](#)
- [BE10A] ———, *SU(2)-Monopoles, Curves with Symmetries and Ramanujan's Heritage*, *Matem. Sbornik* **201** (2010) 19–74.
- [BE10B] ———, *Some remarks on the Ercolani-Sinha construction of monopoles*, *Teor. Mat. Fiz*, 2010, *in press*.
- [BM88] Jean-Benoît Bost and J F Mestre, *Moyenne Arithmético-géométrique et Périodes des Courbes de genre 1 et 2*, *Gaz.Math.S.M.F.* (1988), 36–64.
- [Bra10] H. W. Braden, *Cyclic Monopoles, Affine Toda and Spectral Curves*, [arXiv:1002.1216](#)
- [CG81] E. Corrigan and P. Goddard, *An n monopole solution with 4n – 1 degrees of freedom*, *Commun. Math. Phys.* **80** (1981), 575–587.
- [Cox84] David Cox, *The Arithmetic-Geometric Mean of Gauss*, *L'Enseignement Mathématique* **30** (1984), 275–330.
- [ES89] N. Ercolani and A. Sinha, *Monopoles and Baker Functions*, *Commun. Math. Phys.* **125** (1989), 385–416.
- [FK80] H. M. Farkas and I. Kra, *Riemann Surfaces*, Springer-Verlag, New York, 1980.
- [Fay73] J. D. Fay, *Theta functions on Riemann surfaces*, *Lectures Notes in Mathematics* (Berlin), vol. 352, Springer, 1973.
- [Gau99] C. F. Gauss, *Arithmetisch Geometrisches Mittel*, In *Werke*, Vol. 3, 361–432, Konigliche Gesellschaft der Wissenschaft, Göttingen, 1799.
- [GH78] P. Griffiths and J. Harris, *Principles of Algebraic Geometry*, Wiley, New York, 1978.
- [Hit82] N. J. Hitchin, *Monopoles and Geodesics*, *Commun. Math. Phys.* **83** (1982), 579–602.

- [Hit83] ———, *On the Construction of Monopoles*, Commun. Math. Phys. **89** (1983), 145–190.
- [Hit90] ———, *Harmonic maps from a 2-torus to the 3-sphere*, J. Differential Geom. **31** (1990), 627–710.
- [HMM95] N. J. Hitchin, N. S. Manton and M. K. Murray, *Symmetric monopoles*, Nonlinearity **8** (1995), 661–692.
- [HMR00] C. J. Houghton, N. S. Manton, and N. M. Romão, *On the constraints defining BPS monopoles*, Commun. Math. Phys. **212** (2000), 219–243. arXiv: hep-th/9909168, 1999.
- [Hum01] G. Humbert, *Sur la Transformation Ordinaire des Fonctions Abéliennes*, J. de Math. **7**(5) (1901).
- [KMMZ] V.A.Kazakov, A.Marshakov, J.A.Minahan, K.Zarembo, *Classical/quantum integrability in AdS/CFT* arXiv:hep-th/0402207
- [MS04] Nicholas Manton and Paul Sutcliffe, *Topological Solitons*, Cambridge University Press, Cambridge 2004.
- [Nah82] W. Nahm, *The construction of all self-dual multimonopoles by the ADHM method*, in Monopoles in Quantum Field Theory, edited by N.S. Craigie, P. Goddard and W. Nahm (World Scientific, Singapore 1982).
- [OR82] L.O’Raifeartaigh and S. Rouhani, *Rings of monopoles with discrete symmetry: explicit solution for $n=3$* , Phys. Lett. **112B** (1982) 143.
- [Ric36] F. Richelot, *Essai sur une Méthode Générale pour Déterminer la Valeur des Intégrales Ultra-elliptiques, Fondé sur les Transformations Remarquables de ces Transcendants*, C. R. Acad. Sc. Paris **2** (1836), 622–627.
- [Ric36] F. Richelot, *De transforme Integralium Abelianorum Primi Ordinis Commentation*, J. reine angew. Math. **16** (1837), 221–341.
- [SV04] Tanush Shaska and Helmut Völklein, *Elliptic subfields and automorphisms of genus 2 function fields*, in Algebra, arithmetic and geometry with applications (West Lafayette, IN, 2000) 703–723, Springer Berlin, 2004.
- [Sut97] Paul M. Sutcliffe, *Cyclic Monopoles*, Nucl.Phys. **B505** (1997) 517-539. arXiv:hep-th/9610030

SCHOOL OF MATHEMATICS, EDINBURGH UNIVERSITY, EDINBURGH.

E-mail address: hwb@ed.ac.uk

SCHOOL OF MATHEMATICS, EDINBURGH UNIVERSITY, EDINBURGH.

E-mail address: a.davanzo@ed.ac.uk

INSTITUTE OF MAGNETISM, NATIONAL ACADEMY OF SCIENCES OF UKRAINE.

E-mail address: vze@ma.hw.ac.uk